IEEE Access
Multidisciplinary ⋮ Rapid Review ⋮ Open Access Journal

Received 21 January 2023, accepted 12 February 2023, date of publication 24 February 2023, date of current version 7 March 2023.

Digital Object Identifier 10.1109/ACCESS.2023.3248800

RESEARCH ARTICLE

A Generalized Multiobjective Reliability Redundancy Allocation With Uncertainties

ZUBAIR ASHRAF[1], MOHAMMAD SHAHID[2], (Member, IEEE), FAISAL AHAMD[3], MOHAMMAD SAJID[4], KETAN KOTECHA[5], AND SHRUTI PATIL[5]

[1]Department of Computer Engineering and Application, GLA University, Mathura, Uttar Pradesh 281406, India
[2]Department of Commerce, Aligarh Muslim University, Aligarh 202002, India
[3]Workday Inc., Pleasanton, CA 94588, USA
[4]Department of Computer Science, Aligarh Muslim University, Aligarh 202002, India
[5]Symbiosis Institute of Technology, Symbiosis International (Deemed) University, Pune 412115, India

Corresponding authors: Ketan Kotecha (director@sitpune.edu.in) and Mohammad Shahid (mdshahid.cs@gmail.com)

This work was supported in part by Symbiosis International (Deemed University), Pune, India.

ABSTRACT Multiobjective reliability-redundancy allocation problem (MORRAP) needs to maximize system reliability and minimize cost, weight, and volume with underlining constraints. In the systems' design and analysis phase, uncertainties can occur from various sources, such as manufacturing variability, environmental conditions, user behavior, etc. To deal with this, we present a generalization of the traditional MORRAP under multiple empirical and ambiguous circumstances, named interval type-2 fuzzy multiobjective reliability redundancy allocation problem (IT2FMORRAP). The newly formulated IT2FMORRAP considers optimizing goals as reliability, cost, and weight for a series-parallel system with interval type-2 fuzzy number. The mathematical formulation is established under which the proposed IT2FMORRAP model reduces to T1FMORRAP (type-1 fuzzy MORRAP), IVMORRAP (interval-valued MORRAP), and classical MORRAP. An Enhanced Karnik-Mendel and NSGA-II algorithm-based solving strategy is developed for the proposed IT2FMORRAP. The real-world dataset is considered to demonstrate the efficacy of the solution method for the proposed problem. A K-mean clustering technique identifies the best solution sets from the knee region of the generated Pareto fronts. An experimental study on commonly used performance metrics reveals that IT2FMORRAP performs significantly better than T1FMORRAP and crisp MORRAP. Further, the statistical analysis also confirms the hypothesis established in the empirical research. Finally, a comparative performance study has been conducted with notable state-of-the-art papers from the literature to encounter an appropriate establishment for the proposed work in the domain.

INDEX TERMS Multi-objective reliability optimization, type-2 fuzzy reliability, type-2 fuzzy cost, type-2 fuzzy weight, NSGA-II, k-mean clustering.

I. INTRODUCTION

Reliability optimization is a prominent investigation issue in the design and engineering discipline that has earned massive attention over the last several decades. Reliability refers to its propensity to perform accurately throughout a particular time. The most well-known method of enhancing system reliability is redundancy which concerns the surplus of extra components in the system. Component redundancies, therefore, are connected to unnecessary expenditures of rise in cost, weight, volume, etc., from the perspective of model development. As a result, systems designers put tremendous effort into developing solutions that smack the ideal balance of redundancies and reliability. Researchers have used a variety of methodologies over the decades to determine the optimal reliability and redundancy trade-off, and the issue has come to be acknowledged as the reliability redundancy allocation problem (RRAP) [1], [2].

MORRAP (multiobjective RRAP) seeks to optimize total reliability, weight, and cost with optimal reliability and redundancies, were one goal conflicts with another [2]. Although different system configurations were taken into

The associate editor coordinating the review of this manuscript and approving it for publication was Gustavo Olague.

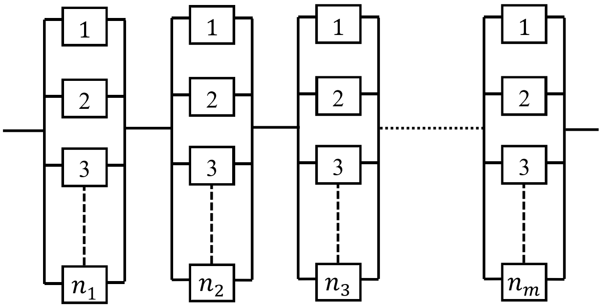

FIGURE 1. Series-parallel systems.

consideration by researchers to examine MORRAP, recently, research studies have primarily focused on the m states series parallel design as shown in Fig. 1. An m states series-parallel configuration has independent m subsystems in series, and each subsystem has n_i $(i \in 1, 2, \ldots m)$ parallelly engineered components, as depicted in Fig. 1. A subsystem is in an active state even if some of its components are not functioning since they provide the same functionality.

The members of subsystems are frequently non-repairable, with two conceivable conditions, functional or non-functional. The operational conditions of the component's reliability are understood, defined, and autonomous. That implies the loss of an individual component does not harm the functional capabilities of the corresponding subsystem or the entire functioning of the system. Nevertheless, there are several empirical uncertainties built into the component reliability of the system that needs to be addressed [3]. Sources of the uncertainties in the subsystem are due to the facts listed as follows:

- The reliability of a device is strongly affected by the environment under which the system is operating. Therefore, it is almost impossible to estimate the exact quantitative value representing the system's reliability, cost, and weight.
- Possibly, the redundant modules may be of various models (materials used by manufacturers) and lack critical information regarding the reliability, cost, and weight needed to evaluate component parameters.
- During the design process, it is difficult to identify the number of redundant modules that can be chosen in a subsystem to ensure superior outcomes for the system.
- System designers have no definite idea about the parameters, viz., cost, volume, and weight, during design. Consequently, they have only guessed and used the estimated values for designing decisions. These estimations are typically based on imprecise, incomplete, and insufficient knowledge.

Therefore, it is essential to use suitable techniques for managing such uncertainties and improving system modeling. These uncertainties are a rudimentary aspect of the modeling that has been unseen lately. Thus, the realistic construction of MORRAP necessitates the deliberation of such empirical uncertainties associated with parameters as they have a serious impact on the modeling framework. These uncertainties in the component parameters of the system are modeled as fuzzy quantities [4] by several researchers [5], [6], [7]. Because these inconsistencies in the component characteristics affect the goals, such as reliability, cost, weight, volume, and so on, the realistic construction of MORRAP demands that these uncertainties be taken into consideration. Several studies [5], [6], [7] represent these uncertainties as fuzzy quantities. However, the type-1 fuzzy numbers (T1FNs) are an inefficient approach to managing the uncertainty from the multiple sources of the system. It is because T1FNs have severe interpretability issues and inaccuracies, and the membership values of T1FNs are crisp. So, they cannot be used to model the higher-order uncertainties [8], [9], [10].

Type 2 Fuzzy Numbers (T2FNs) are an extension of T1FNs that allow for a more precise representation of uncertainty [11]. A T1FN is defined by a membership function that assigns a degree of membership between 0 and 1 to each element of the universe of discourse, whereas a T2FN is defined by a primary membership function and a secondary membership function that assign degrees of membership, respectively, between 0 and 1 to each element of the universe of discourse. It is a fact that the researcher intends to use another variety of T2FS called interval type-2 fuzzy set (IT2FS) due to the high computational effort of T2FS. A T2FS is converted to the IT2FS whenever the level of secondary association functions is equivalent to one. Several other researchers have carried out significant contributions [8], [12], [13], [14], [15] and made this concept a magnificent field of study. Interval type-2 fuzzy numbers (IT2FNs) can discourse the weakness of T1FNs while the degree of belongingness is also demarcated with a type-1 fuzzy illustration [3], [16], [17], [18], [19], [20], [21]. Therefore, the main reasons for taking IT2FNs into account for modeling the component characteristics in MORRAP may be summed up as follows:

a) Subsystems may include components from several suppliers and be constructed using raw resources of mixed qualities. So, the cost, weight, and reliability parameters of the connected components used in separate subsystems may differ.
b) Additionally, design engineers of a specific system could only have a limited understanding of the potential attributes for such component attribute values throughout the designing process. They must provide exact values for the characteristics of the parameters, which they rarely do: thus, they used only approximated values. Therefore, IT2 fuzzy quantities are the best option for modeling them.
c) The degree of belongingness of the inherent uncertainties in the costs, weight, and reliability components may modify according to the perceptions of decision-makers.

So, IT2FNs become the most appropriate to model the scenario In this paper, an IT2FMORRAP is planned to exploit reliability and simultaneously diminish the cost and weight of a series-parallel configuration. With intention parameters as IT2FNs, we highlighted circumstances wherever the theoretical IT2FMORRAP paradigm transforms to T1FMORRAP with T1FNs, IVMORRAP with interval-value (IV) numbers, and MORRAP with crisp or real numbers. Further, IT2FMORRAP, T1FMORRAP, and crisp MORRAP have indeed been addressed by using NSGA-II-based solvent procedures. The dataset of a pharmaceutical plant is being used to examine the solution strategy's effectiveness for perceived cases. A k-mean classification representation is also used to locate the highest quality solution sets from the produced Pareto optimal solutions. The major contribution and motivations of this work are as follows:

1) Proposed a novel Multi-Objective Reliability Redundancy Allocation Problem (MORRAP) using Interval Type-2 Fuzzy Numbers (IT2FN) for modeling uncertainties namely, IT2FMORRAP.
2) The IT2FMORRAP optimizes three objectives simultaneously, such as reliability, cost, and weight of a series-parallel system.
3) The underlining situations are established under which the proposed model abridges to T1FMORRAP, which consider with IVMORRAP, which finally eases to classical MORRAP.
4) A novel solution approach is proposed using the Enhance Karnik-Mendel algorithm and NSGA-II.
5) Experimental simulations are conducted, and results demonstrate that the proposed IT2FMORRAP is superior to that of T1FMORRAP and crisp MORRAP.
6) A k-mean clustering technique is used to recognize the most suited solution region of the optimal Pareto fronts, and indicators, namely, the number of solutions, spacing, spread, diversity, hypervolume, and normalized hypervolume performance, are applied to compare the formulations.
7) Statistical analysis also confirms the hypothesis established in the experimental study.
8) A simulation study along with comparative performance analysis with some other state of art methods from the literature has been conducted.

The remaining work is prepared as follows: An related study of the research work has been given in Section II. Section III presents the mathematical preliminaries. Section IV describes the formulation of the proposed model and its exceptional cases. Section V explains the problem-solving strategy. Section VI has examined the simulation findings and comparative analyses are presented in Section VII. Section VIII is where the paper is concluded.

II. LITERATURE REVIEW

This section will briefly address the research works on the approaches described in this paper. Two subsections cover current IT2FS and reliability optimization studies.

A. INTERVAL TYPE-2 FUZZY SET AND APPLICATIONS

Many situations arise in daily life in which there are more than two choices needed to be considered while making a decision. Solving problems of such kind requires considering more than two possible truth values. Thus, binary yes/no is insufficient for these circumstances, and complex representations are needed. In 1965, Zadeh presented the fundamental concept of fuzzy sets (T1FSs) [4]. The T1FS's uncertainties make it difficult to calculate the precise degree of belongingness. To get around this, Zadeh devised the idea of T2FSs. After that, an IT2FS was described as a unique mathematical formulation of T2FS by assuming a uniform secondary degree [8], [13], [22]. The higher-order IT2FSs expand the range of uncertainties that can be addressed in real-time and broaden the applications. IT2FSs have been used in a variety of applications, including control systems, decision-making, inventory system, pattern recognition, and image processing [16], [23], [24]. IT2FSs are more effective than T1FNs in many cases, particularly in situations where the uncertainty is high or the data is imprecise.

Recently, Ashraf et al. [16] developed an interval type-2 fuzzy logic-based image steganographic system. Ashraf et al. [25] proposed a non-linear system, IT2 vendor-managed inventory system, and solve it with EKM with particle swarm optimization algorithms. IT2 fuzzy neural networks and grasshopper optimization algorithms were suggested by Amirkhani et al. [26] for the development of a vehicle antilock braking system. A robust single fuzzifier IT2 fuzzy C-means clustering method to adopt the interval-valued numbers for the application of land cover segmentation was presented by Wu and Gao [27]. Ashraf and shahid [28] established the multiobjective vender managed model with IT2FNs for demand and order quantity. Javanmard et al. [29] demonstrated a fuzzy solution to a linear programming problem where all coefficients are understood by IT2 FNs. The closest interval approximation is the foundation of the suggested approach.

B. RELIABILITY OPTIMIZATION

Finding the best component redundancy distribution while maximizing reliability is one of the fundamental issues in reliability theory. The early studies on reliability optimization, a dynamic allocation technique [30], and a heuristic technique [31] were presented to determine the best reliability allocation. In a landmark study, M. S. Chern [32] showed that the reliability with redundancies optimization problem is essentially an NP-hard. It motivated the computational intelligence community to compare heuristic-based techniques for RRAP to conventional methodologies such as genetic algorithm (GA) [30] and [33], enhanced GA [34], particle swarm optimization (PSO) [35], [36], bee colony algorithm [37], cuckoo search algorithm with GA [38], imperialist competitive algorithm [39], co-evolutionary differential method with harmony search [40], Gradient-based optimizer [41] and so on.

To solve MORRAP, Coit et al. [42] combined multi-objective optimization problems into a single objective problem. Sheikhalishahi et al. [43] employed a mix of two algorithms, the GA and PSO methods, to enhance reliability by decreasing the cost, weight, and volume under nonlinear constraints. The NSGA strategy was used by Taboada et al. to solve MORRAP [44]. With the universal moment generating function approach for reliability or availability indices, Taboada et al. [45] addressed the multiple objective multi-state RPAP. Under constraints, reliability and cost by NSGA-II are the two goals of Wang et al. [46] reliability optimization model. A multiple-objective evolutionary method for addressing conditions was used by Salazar et al. [47] to solve MORRAP. A knowledge-based simulated annealing approach to solve MORRAP was published by Zaretalab et al. [48]. Cao et al. created the decomposition-based technique in [49] to solve the MORRAP.

To address the issue of uncertain reliability allocation, Gupta et al. [50] used the interval-valued reliability of the components. Under many restrictions, Sahoo et al. [51] solved MORRAP with interval-valued component reliability. An interval-based MORRAP was developed by Zhang et al. [52] and solved using MOPSO. To model the MORRAP and provide a solution, Roy et al. [53] well-thought-out the interval number for the reliability parameters. A fuzzy MORRAP for series-parallel systems was developed by Garg and Sharma [6] utilizing linear and non-linear membership functions, and it was then solved using PSO. When examining the MORRAP, Ebrahimipour and Sheikhalishahi [54] considered a triangular T1FN. Jiansheng et al. [55] addressed MORRAP with unknown parameters like repair rate, failure rate, and other related coefficients in the repairable mode of series-parallel systems.

A fuzzy MORRAP in a type-2 fuzzy environment was first developed by Ashraf et al. [56]. Ashraf et al. [57] presented a PSO-based solution method to solve the type-2 fuzzy MORRAP model. Muhuri et al. [21] constructed an interval type-2 fuzzy reliability of the component-based model for MORRAP, which was solved using the KM and NSGA-II methods. Chebouba et al. [58] solve the multiobjective system reliability of fuzzy quantities using the non-sorting genetic algorithms (NSGA-III). To describe the series-parallel and parallel-series systems, Ashraf et al. [59] presented an IT2 Fuzzy membership function, EKM and PSO were used to solve the formulated interval type-2 fuzzy MORRAPs, and the outcomes were compared to GA.

III. MATHEMATICAL PRELIMINARIES

This section provides descriptions of the essential fundamental terms and techniques [9], [13], [15] used in our proposed problem formulation.

1) A type-2 fuzzy set (T2 FS) $\tilde{\tilde{A}}$ is distinguished by the second-ordered grade of belongingness $\mu_{\tilde{\tilde{A}}}(x, u)$ and

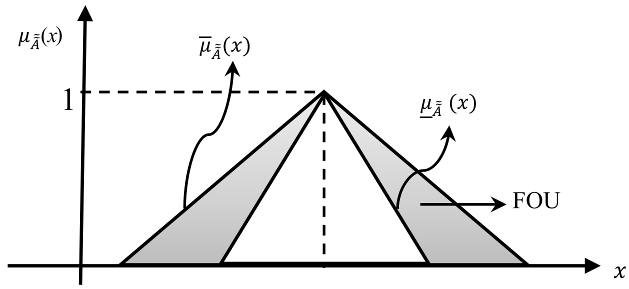

FIGURE 2. IT2FN.

mathematically interpreted as follows.

$$\tilde{\tilde{A}} = \left\{(x, u), \mu_{\tilde{\tilde{A}}}(x, u) \,|\forall x \in X, \forall u \in J_x \subseteq [0, 1]\right\} \quad (1)$$

Here, x represents the principal component considered from the discourse of universe X, and u represents the secondary component function, that is, $u \in J_x \subseteq [0, 1]$. For each element $x \in X$, J_x describes the primary degree of belongingness of x and $\mu_{\tilde{\tilde{A}}}(x, u)$ provides the secondary order degree of belongingness also called the type-2 membership function (T2 MF), such that $0 \leq \mu_{\tilde{\tilde{A}}}(x, u) \leq 1$.

2) An interval type-2 fuzzy set (IT2 FS) $\tilde{\tilde{A}}$, is a T2 FS with the secondary order degree of belongingness $\mu_{\tilde{\tilde{A}}}(x, u)$ is equality and expressed as:

$$\tilde{\tilde{A}} = \left\{(x, u), \mu_{\tilde{\tilde{A}}}(x, u) = 1|\forall x \in X, \forall u \in J_x \subseteq [0, 1]\right\} \quad (2)$$

A closed area under IT2 MFs of an IT2 FS $\tilde{\tilde{A}}$ represents the amount of uncertainty known as the footprint of uncertainty (FOU) and is defined

$$FOU\left(\tilde{\tilde{A}}\right) = \bigcup_{x \in X} J_x^u$$

The inferior and superior of FOU $\left(\tilde{\tilde{A}}\right)$ are defined as follows.

$$\underline{\mu}_{\tilde{\tilde{A}}}(x) = inf\left\{u|u \in [0, 1], \mu_{\tilde{\tilde{A}}}(x, u) > 0\right\} \quad (3)$$

$$\overline{\mu}_{\tilde{\tilde{A}}}(x) = sup\left\{u|u \in [0, 1], \mu_{\tilde{\tilde{A}}}(x, u) > 0\right\} \quad (4)$$

Fig. 2 displays the visual illustration of an IT2 FS $\tilde{\tilde{A}}$.

$$FOU\left(\tilde{\tilde{A}}\right) = [\underline{\mu}_{\tilde{\tilde{A}}}(x), \overline{\mu}_{\tilde{\tilde{A}}}(x)] \quad (5)$$

IV. PROBLEM FORMULATION

This section explains the mathematical framework. The new IT2FMORRAP will be designed. Additionally, it is proved that T1FMORRAP, IVMORRAP, and MORRAP are all particular circumstances of IT2FMORRAP. Table 1 exhibits symbols and abbreviations. Muhuri et al. [21], Kuo et al. [60], Coit and Konak. [42], and Ashraf et al. [57], describe the formulations for the traditional series parallel $m-$ stage framework. In [21], Muhuri et al. considered a structure function χ over a $n-$dimensional space, such that

$\chi = \chi(X); X = (x_1, x_2, \ldots, x_n)$. Now, the nature of $(x_1, x_2, \ldots, x_n)$ decides the nature of structure function (χ), whether it is crisp numbers, interval-value numbers, T1FNs, or IT2FNs. For a $m-$stage series-parallel configuration, as presented in Fig. 1, the chrematistics of each elements are assumed to be defined and autonomous. Thus, the total reliability function $\tilde{\tilde{R}}_S$ corresponding to IT2 fuzzy reliabilities $\tilde{\tilde{r}}_1, \tilde{\tilde{r}}_2, \ldots, \tilde{\tilde{r}}_n$, can be constructed by using the structural function as mentioned above presented in Eq. (6):

$$\tilde{\tilde{R}}_S = \chi\left(\tilde{\tilde{r}}_1, \tilde{\tilde{r}}_2, \ldots, \tilde{\tilde{r}}_n\right) \tag{6}$$

Here, $\tilde{\tilde{r}}_i$ are represented with IT2FNs. An IT2FN has been represented by a triangular IT2MF $(\mu_{\tilde{\tilde{r}}_i})$ which is actually a set value mapping with respect to IT2 fuzzy reliability $\tilde{R}_s(x_i) = \{1-\mu_{f_t}(r_i n_i)\}\tilde{r}_i$, can be defined as follows:

$$\mu_{\tilde{\tilde{r}}_i}(x) = \begin{cases} 0, & x \le r_{left}^{up} \\ \dfrac{x - r_{left}^{up}}{r_s - r_{left}^{up}}, & r_{left}^{up} \le x \le r_{left}^{lo} \\ \left[\dfrac{x - r_{left}^{up}}{r_s - r_{left}^{up}}, \dfrac{x - r_{left}^{lo}}{r_s - r_{left}^{lo}}\right], & r_{left}^{lo} \le x \le r_s \\ \left[\dfrac{r_{right}^{lo} - x}{r_{right}^{lo} - r_s}, \dfrac{r_{right}^{up} - x}{r_{right}^{up} - r_s}\right], & r_s \le x \le r_{right}^{lo} \\ \dfrac{r_u^r - x}{r_u^r - r_s}, & r_{right}^{lo} \le x \le r_{right}^{up} \\ 0, & x \ge r_{right}^{up} \end{cases} \tag{7}$$

where r_{left}^{up} and r_{right}^{up} are left and right extreme points of the upper membership function (UMF). Similarly, r_{left}^{lo}, and r_{right}^{lo} are left and right extreme points of lower membership function (LMF) (see Fig. 3). So, overall system reliability $\tilde{\tilde{R}}_S\left(\tilde{\tilde{r}}, n\right)$, IT2 fuzzy cost $\tilde{\tilde{C}}_S\left(\tilde{\tilde{r}}, n\right)$, IT2 fuzzy volume $\tilde{\tilde{V}}_S\left(\tilde{\tilde{w}}, n\right)$ and IT2 fuzzy weight and $\tilde{\tilde{W}}_S\left(\tilde{\tilde{w}}, n\right)$ of $m-$stage system configuration [21] is mathematically represented as:

$$\tilde{\tilde{R}}_S\left(\tilde{\tilde{r}}, n\right) = \prod\nolimits_{i=1}^{m}\left[1 - (1-\tilde{\tilde{r}}_i)^{n_i)}\right] \tag{8}$$

$$\tilde{\tilde{C}}_S\left(\tilde{\tilde{r}}, n\right) = \sum\nolimits_{i=1}^{m}\left[\alpha_i\left(-\frac{t}{\ln\left(\tilde{\tilde{r}}_i\right)}\right)^{\beta_i}.(n_i + exp(n_i/4))\right] \tag{9}$$

$$\tilde{\tilde{V}}_S\left(\tilde{\tilde{r}}, n\right) = \sum\nolimits_{i=1}^{m}\tilde{\tilde{w}}_i v_i^2 n_i^2 \tag{10}$$

$$\tilde{\tilde{W}}_S\left(\tilde{\tilde{r}}, n\right) = \sum\nolimits_{i=1}^{m}\tilde{\tilde{w}}_i.(n_i * exp(n_i/4)) \tag{11}$$

Thus, IT2FMORRAP may be formulated as:

$$\begin{aligned} &\text{Maximize}\widetilde{\widetilde{R_S}}\left(\tilde{\tilde{r}}, n\right), \\ &\text{Minimize}\widetilde{\widetilde{C_s}}\left(\tilde{\tilde{r}}, n\right), \\ &\text{Minimize}\widetilde{\widetilde{W_s}}\left(\tilde{\tilde{r}}, n\right) \\ &\text{Subject to } \tilde{\tilde{V}}_s\left(\tilde{\tilde{r}}, n\right) \end{aligned} \tag{12}$$

TABLE 1. List of notations/symbols used in the model.

Notation	Description	Notation	Description
i	Index of i–th subsystem	m	Number of subsystems
n_i	Number of components i–th subsystem	α_i, β_i	Shaping and scaling factors of i–th subsystem
r_i	Component reliability of i–th subsystem	v_i	Component volume of i–th subsystem
w_i	Component weight of i–th subsystem	$\tilde{r}_i$	Type-1 (T1) fuzzy reliability
$\tilde{\tilde{r}}_i$	IT2 (interval type-2) fuzzy reliability	$r_{i_{left}}, r_{i_{irig}}$	Left and right extremists of reliability in MF
$r_{i_{left}}^{up}, r_{i_{right}}^{up}$	Left and right extremists of reliability in Upper MF	$r_{i_{left}}^{lo}, r_{i_{righ}}^{lo}$	Left and right extremists of reliability in Lower MF
$\tilde{w}_i$	T1 fuzzy of weight	$\tilde{\tilde{w}}_i$	IT2 fuzzy weight
$w_{i_{left}}, w_{i_{irig}}$	Left and right extremists of weight in MF	$w_{i_{left}}^{up}, w_{i_{ri}}^{up}$	Left and right extremists of weight in Upper MF
$w_{i_{left}}^{lo}, w_{i_{rig}}^{lo}$	Left and right extremists of weight in Lower MF	R_s	Reliability of the system
C_s	Cost of the system	V_s	Volume of the system
W_s	Weight of the system	$\tilde{R}_s$	T1 fuzzy system's reliability
$\tilde{C}_s$	T1 fuzzy system's cost	$\tilde{V}_s$	T1 fuzzy system's volume
$\tilde{W}_s$	T1 fuzzy system's weight	$\tilde{\tilde{R}}_s$	IT2 fuzzy system's reliability
$\tilde{\tilde{C}}_s$	IT2 fuzzy system's cost	$\tilde{\tilde{W}}_s$	IT2 fuzzy system's weight
$\tilde{\tilde{V}}_s$	IT2 fuzzy system's volume	t	Temperature of the system
C	Upper limit of the total system cost	W	Upper limit of system weight
V	Upper limit of volume		

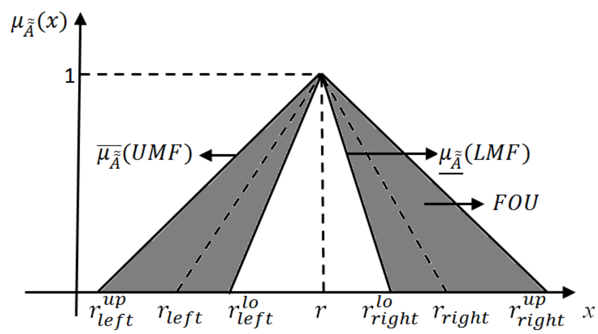

FIGURE 3. Interval Type-2 Triangular Fuzzy Number.

In special cases, generalized IT2FMORRAP presented by Eq. (13) has been reduced to T1FMORRAP, IVMORRAP, and MORRAP, as discussed in the following cases.

A. CASE 1: TIFMORRAP

When, $r_{left}^{lo} = r_{left}^{up}$ and $r_{right}^{lo} = r_{right}^{up}$, IT2FMORRAP condenses to T1FMORRAP, that is, the lest and most bound equivalent to left support $[r_{left}^{up}, r_{left}^{lo}]$ meets to r_{left} as well as the right support $[r_{right}^{lo}, r_{right}^{up}]$ meets to r_{right} (See Fig. 3 and Fig. 4). If $r_{left}^{lo} = r_{left}^{up} = r_{left}$ and $r_{right}^{lo} = r_{right}^{up} = r_{right}$ then, left support and right support converge to point r_{left} and r_{right} respectively and IT2MF $(\mu_{\tilde{\tilde{r}}_i})$ presented in Eq. (7) reduces to

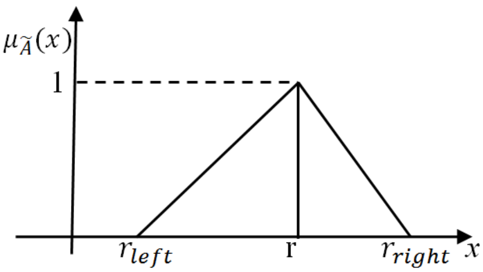

FIGURE 4. Type-1 Fuzzy Number.

a T1MF ($\mu_{\tilde{r}_i}$) as follows:

$$\mu_i(x) = \begin{cases} 0, & x < r_{left} \\ \dfrac{x - r_{left}}{r_s - r_{left}}, & r_{left} \leq x \leq r_s \\ \dfrac{r_s - x}{r_{right} - r_s}, & r_s \leq x \leq r_{right} \\ 0, & x > r_{right} \end{cases} \tag{13}$$

Thus, overall T1 fuzzy reliability $\tilde{R_S}(\tilde{r}, n)$, cost $\tilde{C_S}(\tilde{r}, n)$, weight $\tilde{W_S}(\tilde{w}, n)$ and volume $\tilde{V_S}(\tilde{w}, n)$ can be stated as:

$$\tilde{R_S}(\tilde{r}, n) = \prod\nolimits_{i=1}^{m} \left[1 - (1 - \tilde{r})^{n_i}\right] \tag{14}$$

$$\tilde{C_S}(\tilde{r}, n) = \sum\nolimits_{i=1}^{m} \left[\alpha_i \left(-\frac{t}{\ln(\tilde{r}_i)}\right)^{\beta_i} . \left(n_i + \exp\left(\frac{n_i}{4}\right)\right)\right] \tag{15}$$

$$\tilde{W_S}(\tilde{r}, n) = \sum\nolimits_{i=1}^{m} \tilde{w}_i . \left(n_i * \exp\left(\frac{n_i}{4}\right)\right) \tag{16}$$

$$\tilde{V_S}(\tilde{r}, n) = \sum\nolimits_{i=1}^{m} \tilde{w}_i . v_i^2 n_i^2 \tag{17}$$

Thus, we formulate T1FMORRAP as:

$$\begin{aligned} &\text{Maximize } \widetilde{R_S}(\tilde{r}, n) \\ &\text{Minimize } \widetilde{C_S}(\tilde{r}, n) \\ &\text{Minimize } \widetilde{W_S}(\tilde{w}, n) \\ &\text{Subject to } \widetilde{V_S}(\tilde{w}, n) \end{aligned} \tag{18}$$

B. CASE 2: INTERVAL-VALUED MORRAP

In IT2FMORRAP, the FOU portrait the interval , $I = [I_{left}, I_{right}]$ in which I_{left}andI_{right} are taken from interval s, $\left[r_{left}^{up}, r_{left}^{lo}\right]$ and $[r_{right}^{lo}, r_{right}^{up}]$ respectively. If $r_{left} = r_{left}^{up} = r_{left}^{lo}$ and $r_{right} = r_{right}^{lo} = r_{right}^{up}$, then IT2FN transforms into the T1FN and it is distinct from interval $I' = [r_{left}, r_{right}]$. Additionally, suppose the membership function values as one over the interval points of $I' = [r_{left}, r_{right}]$ therefore, T1FN will express as an interval-valued number as illustrated in Fig. 5. Thus, the IVNORRAP model [52] with total interval-valued reliability $[R_{left}, R_{right}]$ can be expressed follows:

$$[R_{left}, R_{right}] = \prod\nolimits_{i=1}^{m} \left[1 - [1 - r_{i_{left}}, 1 - r_{i_{right}}]^{n_i}\right] \tag{19}$$

Similarly, total interval-valued cost $[C_{left}, C_{right}]$, interval-valued weight $[W_{left}, W_{right}]$ and interval-valued volume $\left[V_{left}, V_{right}\right]$ are expressed as follows:

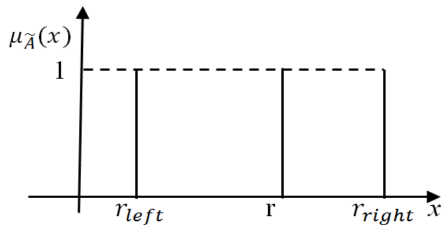

FIGURE 5. Interval Valued Number.

$$\left[C_{\text{left}}, C_{\text{right}}\right] = \sum\nolimits_{i=1}^{m} \left[\alpha_i \left[\frac{t}{\ln(r_{i\ \text{left}})}, \frac{-t}{\ln(r_{i_i\ \text{rght}})}\right]^{\beta_i} \cdot \left(n_i + \exp\left(\frac{n_i}{4}\right)\right)\right] \tag{20}$$

$$\left[W_{\text{left}}, W_{\text{right}}\right] = \sum\nolimits_{i=1}^{m} \left[w_{i_{\text{left}}}, w_{i_{\text{right}}}\right] \cdot \left(n_i * \exp\left(\frac{n_i}{4}\right)\right) \tag{21}$$

$$\left[V_{\text{left}}, V_{\text{right}}\right] = \sum\nolimits_{i=1}^{m} \left[w_{i_{\text{left}}}, w_{i_{\text{right}}}\right] \cdot v_i^2 n_i^2 \tag{22}$$

Thus, the interval-valued MORRAP is:

$$\begin{aligned} &\text{Maximize } \left[R_{\text{left}}, R_{\text{right}}\right] \\ &\text{Minimize } \left[C_{\text{left}}, C_{\text{right}}\right] \\ &\text{Minimize } \left[W_{\text{left}}, W_{\text{right}}\right] \\ &\text{Subject to } \left[V_{\text{left}}, V_{\text{right}}\right] \end{aligned} \tag{23}$$

C. CASE 3: CRISP MORRAP

Finally, the T1FMORRAP will present a MORRAP when $r_{left} = r_{right} = r_s$, as the classical number is shown in Fig. 6 because of the degree of belonging $\mu_{\tilde{r}_i}(x)$ will be present by the characteristic function $\zeta_{r_i}(x)$:

$$\zeta_s(x) = \begin{cases} 1 x = r_s \\ 0 \textit{ otherwise} \end{cases} \tag{24}$$

Therefore, MORRAP [60] is:

$$\text{Maximize } R_s(r, n) = \prod_{i=1}^{m} \left[1 - (1 - r_i)^{n_i}\right]$$

$$\text{Minimize } C_s(r, n) = \sum_{i=1}^{m} \left[\alpha_i \left(-\frac{t}{\ln(r_i)}\right)^{\beta_i} \cdot (n_i + exp(n_i/4))\right]$$

$$\text{Minimize } W_s(w, n) = \sum_{i=1}^{m} w_i.(n_i * exp(n_i/4))$$

$$\text{Subject to } V_s(w, n) = \sum_{i=1}^{m} w_i v_i^2 n_i^2 \tag{25}$$

As per the aforementioned discussion, we finally concluded that the formulation of IT2FMORRAP is a generalized framework for other MORRAP models, Viz. T1FMORRAP [6], IVMORRAP [52], MORRAP [60].

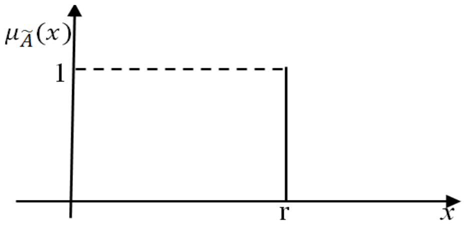

FIGURE 6. Classical number.

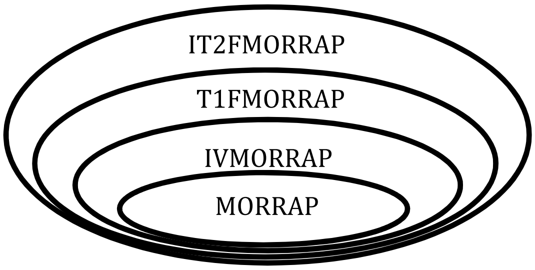

FIGURE 7. The structural connection amongst the IT2FMORRAP, T1FMORRAP, IVMORRAP, and MORRAP.

The stated argument comes under the cope with Zadeh's detection [10] of the excellent capabilities of fuzzy sets to generalize mathematical models. It is also genuinely agreeable with notable judgments [61], [62], which show crisp sets, interval-valued sets, and type-1 fuzzy sets are special cases of type-2 fuzzy sets. Fig. 7 shows the visual hierarchy among the IT2FMORRAP, T1FMORRAP, IVMORRAP, and crisp MORRAP [21].

V. PROPOSED SOLUTION APPROACH

This section explains the solution approach, which uses the well-known non-dominated sorting genetic algorithm (NSGA-II) suggested by Deb et al. [63] and interval type-2 fuzzy system (IT2FS) [9]. Fig. 8 illustrates the nature of our planned solution strategy. The major processes involved in the approach are discussed as follows.

A. IT2 FUZZIFICATION

Multiple experts opinions on ambiguous decision-making variables leads complexity in the process, leaving scope of IT2 fuzzy systems [15]. IT2 fuzzy systems are employed with IT2 fuzzification to generate IT2FNs), adopted from [21]. Generally, the estimations of decision-makers are a specified range or interval (say I) represented via IT2FNs and may be in any one form i.e. Gaussian, trapezoidal, and triangular functions. Therefore, it requires some logical reasoning to choose best suited IT2MF $\mu_{\tilde{\tilde{A}}}$. As discussed earlier, reliability defines the likelihood of an operational device that will function correctly without any faults, and the time to failure (t) is the most promising value provided by the experts [21], [59]. Therefore, the IT2MF of the reliability at this particular time instance (t) is equivalent to one. In other terms, for $r(t)$, the IT2MF $(\mu_{\tilde{\tilde{r}}})$ should only be one with only one highest value, which also implies that IT2MF is normal. And, for any system that will operate over an endless period is also not feasible. Therefore, an extensive tail with more non-zero values is insignificant after a limit. Hence, neither trapezoidal nor Gaussian functions are suitable choices for modeling IT2FMORRAP. Thus, the triangular function is the best option to model IT2 fuzzy reliability, and weight parameters. It may also be possible that the endpoints of the interval of uncertainty (I), that is, left endpoint ($\mathrm{I_{left}}$) and right endpoint ($\mathrm{I_{right}}$), are uncertain due the multiple range provided by experts. Then, each $\mathrm{I_{left}}$ and $\mathrm{I_{right}}$ will also form the interval with lower bound and upper bounds. Specifically, for component reliability , r, the $\mu_{\tilde{\tilde{r}}}$ will have $\mathrm{r} = [\mathrm{r_{left}}, \mathrm{r_{right}}]$ and each endpoint in interval will have lower and upper bounds, i.e., $\mathrm{r_{left}} = [\mathrm{r_{left}^{up}}, \mathrm{r_{left}^{lo}}]$ and $\mathrm{r_{right}} = [\mathrm{r_{right}^{lo}}, \mathrm{r_{right}^{up}}]$, respectively. The IT2FN of reliability $(\tilde{\tilde{r}})$ with the triangular IT2MF is presented in Eq. (7) and pictorially demonstrated in Fig. 3. A detailed algorithm for the generation of IT2FN with the parameters can be seen in [21].

B. IT2 FUZZY TYPE-REDUCTION AND DEFUZZIFICATION

The type-reduction procedure changes the IT2MFs into T1MFs. T1MFs transform into an output number by using the procedure of defuzzification. Several methods have been developed to perform the type-reduction and defuzzification of IT2 FN. Among them, Enhanced Karnik-Mendel (EKM) algorithm [13] is one of the most commonly used methods for the purpose. EKM algorithm is used for the type-reduction process. The iteration number is kept low to offer an improvement in initializing and terminating situations. A centroid $C_{\tilde{\tilde{A}}}(x)$ is the combination of the centroids of all its embedded T1FSs. That is,

$$C_{\tilde{\tilde{A}}}(x) = \left\{ c_l\left(\tilde{\tilde{A}}\right), \ldots, c_r\left(\tilde{\tilde{A}}\right) \right\} = \left[c_l\left(\tilde{\tilde{A}}\right), c_r(\tilde{\tilde{A}}) \right] \quad (26)$$

The EKM algorithm is divided into two parts: in the first part, the computation of the c_l is performed and in other parts c_r is calculated. Eq. (27) and Eq. (28) are used for computing c_l and c_r.

$$c_l(L) = \left(\sum_{i=1}^{N} x_i\theta_i \Big/ \sum_{i=1}^{N} \theta_i \right) \quad (27)$$

$$c_r(R) = \left(\sum_{i=1}^{N} x_i\theta_i \Big/ \sum_{i=1}^{N} \theta_i \right) \quad (28)$$

The procedure of the EKM algorithm is explained in detail in [9], [16], and [59]; here, the first part is for the algorithm to compute c_l and second one is for evaluating c_r.

The defuzzification will provide the ultimate output number (y_d) corresponding to IT2FN and is the average of the c_l and c_r, as follows:

$$y_d = \frac{c_l + c_r}{2} \quad (29)$$

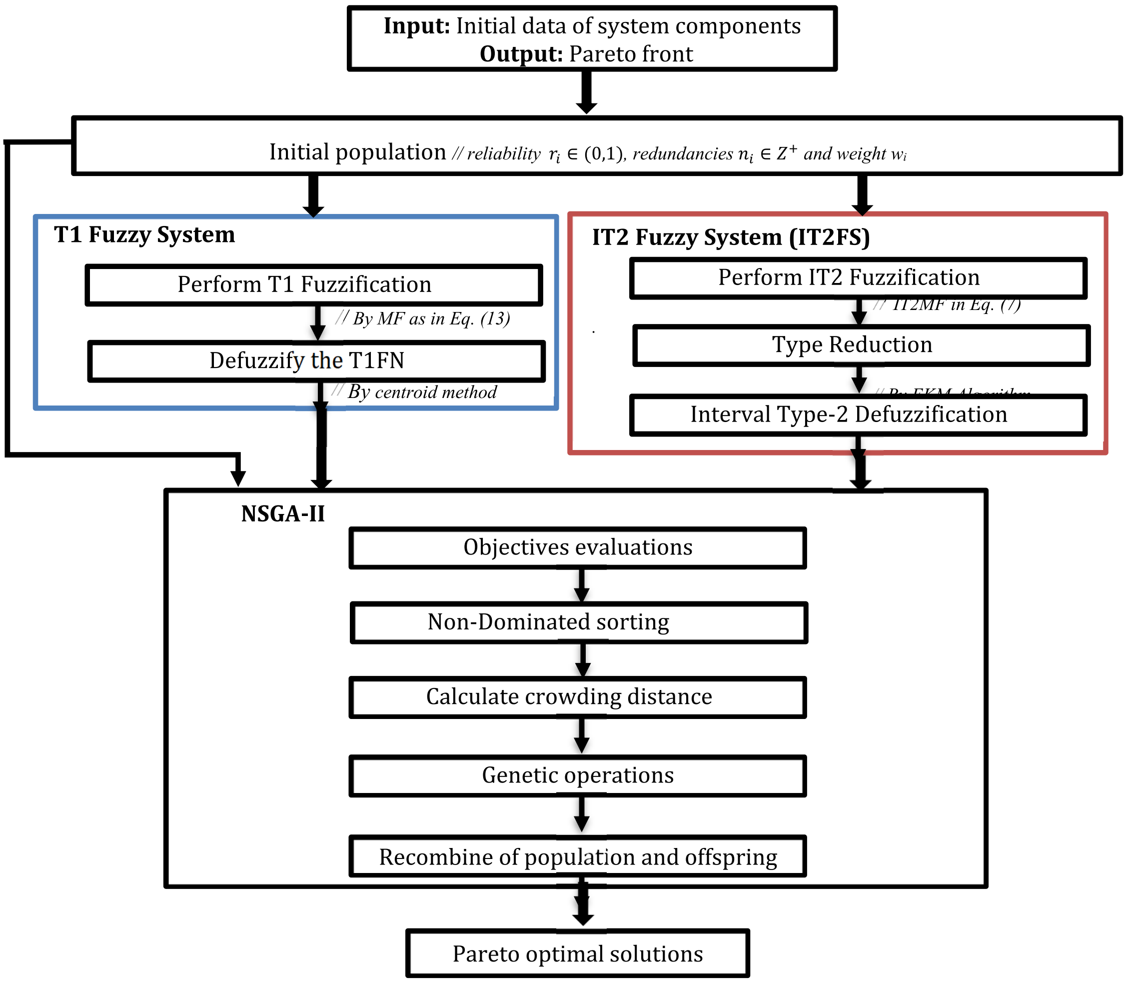

FIGURE 8. The workflow diagram of our implantations suggested a solution approach for solving IT2FMORRAP, T1FMORRAP, and MORRAOP.

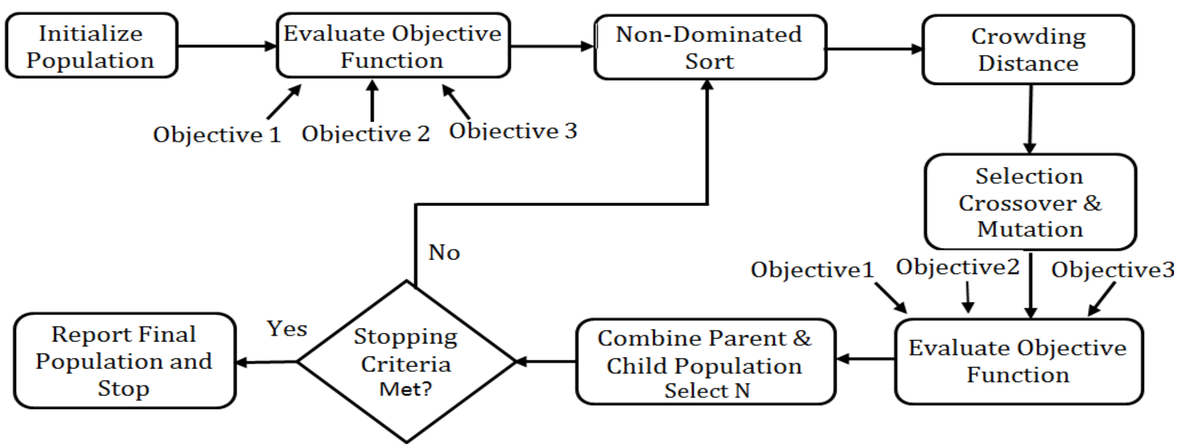

FIGURE 9. Flow chart of NSGA-II.

C. NON-DOMINATED SORTING GENETIC ALGORITHM-II (NSGA-II)

Many scientists widely adopted NSGA-II [63], a multi-objective evolutionary optimization approach to solve various decision-making models with multiple goals. The pictorial representation of NSGA-II is given in Fig. 9. The subsequent sections explain the various sub-procedures of NSGA-II, including three goals, namely, (i) maximize the total

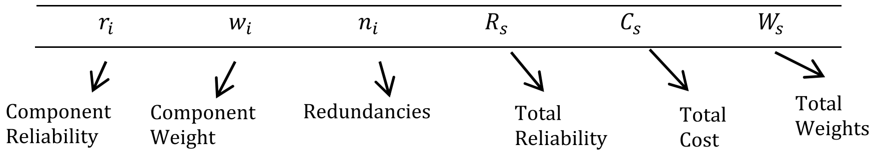

FIGURE 10. Individual or Chromosome Structure.

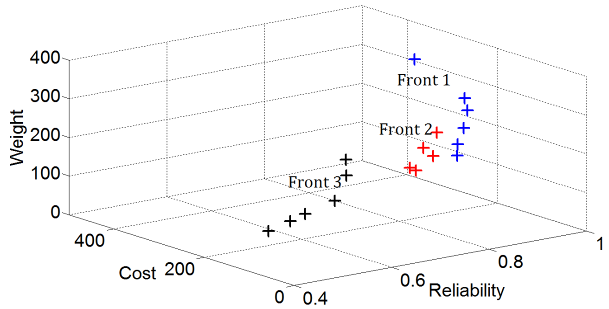

FIGURE 11. Front generated by non-dominate sort.

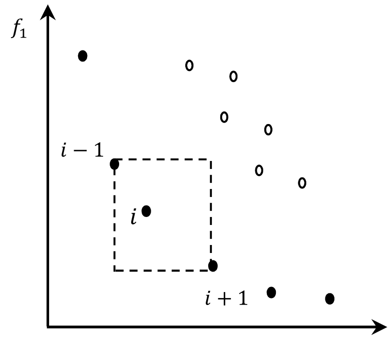

FIGURE 12. Crowding distance.

reliability of the system, (ii) minimize the overall cost of the system (iii) minimize the total weight of the system, under fixed volume and limiting constraints.

1) CHROMOSOME STRUCTURE AND OBJECTIVES EVALUATIONS

A chromosome/genome is an array of genomic sequences represented by floating-points. A genome is a uniformly distributed random solution that lies inside a predefined search space. In IT2FMORRAP, components' reliability (r_i), components' weight (w_i) and the redundant components (n_i) of the $i-th$ subsystem are genes of the chromosome. The variables parameters r_i, w_i, and n_i are of range [0.5, 0.99999], [7.0, 12.0], and [1], [5], respectively. A chromosome structure has been depicted in Fig. 10 to maximize the reliability (R_S), minimize the costs (C_S) and minimize the weight (W_S) of the system. The initialization of the initial population is similar to the original NSGA-II.

2) NON-DOMINATED SORT

The population generated initially has been sorted by a fast non-domination sorting algorithm introduced by Dev et al. [63]. In non-dominated sorting, solution X is supposed to dominate Y if and only if the objectives of X are no worse than the objective of Y and there must exist at least one objective of X, which is better than that of Y [64]. At first, we consider a set S containing all the N individual solutions of the population without losing the generality.

The sorting algorithm will then select the non-dominated solutions from S and assign them to rank-1 and call them Front-1 of the Pareto-front. Again, the left-out solutions of S are sorted, and the non-dominating ones are assigned as rank-2 forming the Front-2. This process repeats until there is no solution left in S to dominate others, and these solutions will create the kth rank Pareto-front as Front $-k$. The Pareto-front for IT2FMORRAP shaped via the non-dominated sorting process with the three objectives is shown in Fig. 11. After sorting and assigning the rank to the fronts, the crowding distance of each front is determined.

3) CROWDING DISTANCE

The difference between individual solutions on the front is measured by the crowding distance depending on the objective function values, as shown in Fig. 12. In a Pareto-Front F_i, the crowding distance (D_{jm}), for each individual $j = 2, 3, \ldots n_i - 1$ and $m = 1, 2, \ldots, M$ number of objectives are arranged in increasing order is calculated as follows:

$$D_{jm} = \frac{(f_m(j+1) - f_m(j-1))}{\left(f_m^{max} - f_m^{min}\right)}, j = 2, 3, \ldots n_j - 1 \quad (30)$$

The overall crowding distance of an individual j is $D_j = \sum_{m=1}^{M} D_{jm}$.

4) GENETIC OPERATIONS

Selection operation: The tournament selection approach is used in the selection process. The population's solutions are adopted by a crowded-comparison operator [65]. The comparative operator guides the selection method using ranks measured in the sorting process and the crowding distance. For a particular individual, if an individual has a lower or the equivalent rank and higher crowding distance, it is said that the comparative operator is more dominant than the other. Solutions are selected to create a mating pool to perform the crossover and mutation procedures to generate the new offspring just after the selection process.

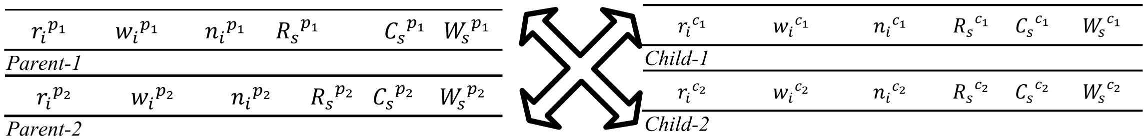

FIGURE 13. **Crossover Operation.**

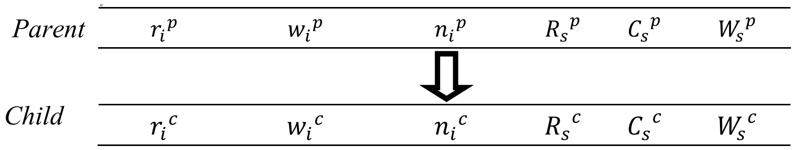

FIGURE 14. **Mutation Operation.**

Crossover: Simulated binary crossover strategies generate child individuals for each parent individual, as shown in Fig. 13. The binary crossover procedure is as follows.

Step-1: Create a randomly generated number u from a range between 0 and 1.

Step-2: Find the spread factor ρ as:

$$\rho = \begin{cases} (2u)^{\frac{1}{(\eta+1)}}, & if\ u \leq 0.5 \\ \dfrac{1}{[2(1-u)]^{\frac{1}{(\eta+1)}}}, & otherwie \end{cases} \tag{31}$$

where, η is a probability index also known as crossover probability.

Step-3: Suppose $par_{1,\mathrm{j}}$,$par_{2,\mathrm{j}}$ be two parents. Now the two children are generated as follows:

$$ch_{1,j} = \frac{1}{2}[(1-\rho) * par_{1,j} + (1+\rho) * par_{2,j}] \tag{32}$$

$$ch_{2,j} = \frac{1}{2}[(1+\rho) * par_{1,j} + (1-\rho) * par_{2,j}] \tag{33}$$

Mutation: the polynomial mutation procedure is used to restore unexpected solutions to prevent getting stuck into the local optimum, resulting in exploration ability and diversity in the population. as demonstrated in fig. 14, a parent par_j with upper bounds ($\mathrm{par}_j^{\mathrm{u}}$) and lower bounds $\left(\mathrm{par}_j^{\mathrm{l}}\right)$, child $\mathrm{ch_j}$ is calculated as:

$$ch_j = par_j + \left(par_j^u - par_j^l\right) * \delta_j \tag{34}$$

$$\delta_j = \begin{cases} (2u)^{\frac{1}{(\eta_m+1)}}, & if\ u < 0.5 \\ 1-[2(1-u)]^{\frac{1}{(\eta_m+1)}}, & otherwie \end{cases} \tag{35}$$

in eq. (34), δ_j is evaluated using eq. (35) where u represents a random number and η_m is mutation probability.

5) RECOMBINATION

In the recombination procedure, the older population and newly-generated offspring are mixed to ensure elitism in the NSGA-II. The current population is then shifted over to non-domination sorting to form the fronts. Suppose, the population size of solutions is more than N number of individuals on the Pareto-front. Then, individuals are sorted using the non-dominated sorting and arranged in decreasing order based on crowding distance to pick the first N solutions. The same is repeated until the stopping criteria are met. The typical illustration of the NSGA-II is pictorially demonstrated in Fig. 15. Finally, NSGA-II effectively establishes the Pareto-front solutions and offers a comprehensive knowledge of multiple optimal solutions over the search space.

The proposed solution model is accomplished by two procedures, namely IT2FS and NSGA-II. The IT2FS consist of three sub-procedures, such as, IT2 fuzzification, type reduction and defuzzification. The time complexity of these procedures for each system components, reliability, cost and weight, are $\mathrm{O}(\mathrm{n})$, $\mathrm{O}(\mathrm{n})$ and $\mathrm{O}(1)$, respectively. Hence, the combined time complexity of IT2FS= $\mathrm{O}(\mathrm{n}) + \mathrm{O}(\mathrm{n}) + \mathrm{O}(1) \simeq O(\mathrm{n})$. Now, the time complexity of NSGAII is $\mathrm{O}(\mathrm{m} \times \mathrm{n} \times \mathrm{n})$, for m objective and n population size. So, the worst-case time complexity for the proposed solution approach is $\mathrm{O}(\mathrm{n}) + \mathrm{O}(\mathrm{m} \times \mathrm{n} \times \mathrm{n}) \simeq \mathrm{O}(\mathrm{mn}^2)$.

VI. EXPERIMENTAL SIMULATIONS

To demonstrate the proposed solution for IT2FMORRAP, we have taken a real application data set of a pharmaceutical factory, presented in Table 2 [6]. The experimental simulations have been conducted on MATLAB 2015b on a processor 3.40 GHz Xeon with 16 GB RAM and a Windows 10 operating system. The IT2FMORRAP formulations in Section IV are mixed-integer MOOPs with nonlinear objectives and constrained functions. Now, the proposed NSGA-II solution approach is applied to solve the given problem as in Table 2.

A. PROBLEM STATEMENTS

With the parameters in Table 2, the formulations of the IT2FMORRAP, T1FMORRAP, and MORRAOP are as given below:

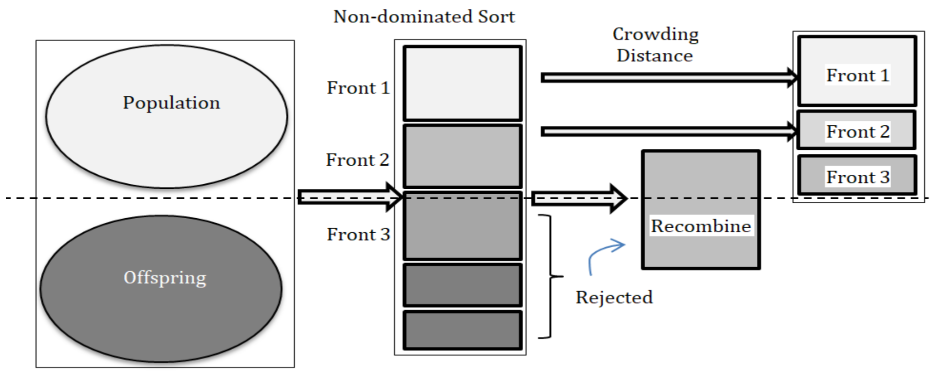

FIGURE 15. Illustration of procedures in separate NSGA-II phases.

TABLE 2. Input Parameter data.

i	$10^5 * \alpha_i$	β_i	w_i	v_i	V	t
1	0.611360	1.5	9.0	4.0		
2	4.032464	1.5	7.0	5.0		
3	3.578225	1.5	5.0	3.0		
4	3.654303	1.5	9.0	2.0		
5	1.163718	1.5	9.0	3.0	289	1000
6	2.966955	1.5	10.0	4.0		
7	2.045865	1.5	6.0	1.0		
8	2.649522	1.5	5.0	1.0		
9	1.982908	1.5	8.0	4.0		
10	3.516724	1.5	6.0	4.0		

1) IT2FMORRAP FORMULATION

$$\text{Maximization } \tilde{\tilde{R}}_S\left(\tilde{\tilde{r}}, n\right) = \prod_{i=1}^{10} \left[1 - (1 - \tilde{\tilde{r}}_i)^{n_i}\right]$$

$$\text{Minimization } \tilde{\tilde{C}}_S\left(\tilde{\tilde{r}}, n\right) = \sum_{i=1}^{10} \left[\alpha_i \left(-\frac{1000}{\ln\left(\tilde{\tilde{r}}_i\right)}\right)^{\beta_i} \cdot \left(n_i + \exp\left(\frac{n_i}{4}\right)\right)\right]$$

$$\text{Minimization } \tilde{\tilde{W}}_S\left(\tilde{\tilde{w}}, n\right) = \sum_{i=1}^{10} \tilde{\tilde{w}}_i . \left(n_i * \exp\left(\frac{n_i}{4}\right)\right)$$

$$\text{Subject to } \sum_{i=1}^{10} \tilde{\tilde{w}}_i v_i^2 n_i^2 \leq 289$$

$$\tilde{\tilde{r}} = \left(\tilde{\tilde{r}}_1, \tilde{\tilde{r}}_2, \ldots, \tilde{\tilde{r}}_{10}\right); \tilde{\tilde{r}}_i = \left[\tilde{r}_{ileft}, \tilde{r}_{iright}\right],$$
$$\tilde{r}_{ileft} = \left[r_{left}^{up}, r_{left}^{lo}\right], \tilde{r}_{iright} = \left[r_{right}^{lo}, r_{right}^{up}\right]'$$
$$r_{left}^{lo}, r_{left}^{up}, r_{right}^{lo}, r_{right}^{up}$$
$$\in [0.1, 0.99999]\, \forall lo, up \in \{1, 2, 3, \ldots, 10\};$$
$$\tilde{\tilde{w}} = \left(\tilde{\tilde{w}}_1, \tilde{\tilde{w}}_2, \ldots, \tilde{\tilde{w}}_{10}\right), \tilde{\tilde{w}}_i = \left[\tilde{e}w_{ileft}, \tilde{w}_{iright}\right],$$
$$\tilde{w}_{ileft} = \left[w_{left}^{up}, w_{left}^{lo}\right], \tilde{w}_{iright} = \left[w_{right}^{lo}, w_{right}^{up}\right],$$
$$w_{left}^{up}, w_{left}^{lo}, w_{right}^{lo}, w_{right}^{up}$$
$$\in [0.7, 12.0]\, \forall lo, up \in \{1, 2, 3, \ldots, 10$$
$$n_i = (n_1, n_2, \ldots, n_{10}) \text{ and } 1 \leq n_i \leq 5.$$

2) T1FMORRAP FORMULATION

$$\text{Maximization } \tilde{R}_S\left(\tilde{r}, n\right) = \prod_{i=1}^{10} \left[1 - (1 - \tilde{r}_i)^{n_i}\right]$$

$$\text{Minimization } \tilde{C}_S\left(\tilde{r}, n\right) = \sum_{i=1}^{10} \left[\alpha_i . \left(-\frac{1000}{\ln\left(\tilde{r}_i\right)}\right)^{\beta_i} \cdot \left(n_i + \exp\left(\frac{n_i}{4}\right)\right)\right]$$

$$\text{Minimization } \tilde{W}_S\left(\tilde{w}, n\right) = \sum_{i=1}^{10} \tilde{w}_i . \left(n_i * \exp\left(\frac{n_i}{4}\right)\right)$$

$$\text{Subject to } \sum_{i=1}^{10} \tilde{w}_i . v_i^2 n_i^2 \leq 289$$
$$\tilde{r} = \left(\tilde{r}_1, \tilde{r}_2, \ldots, \tilde{r}_{10}\right), \tilde{w} = \left(\tilde{w}_1, \tilde{w}_2, \ldots, \tilde{w}_{10}\right),$$
$$\tilde{r}_i = \left[r_{i_{left}}, r_{i_{right}}\right], \tilde{w}_i = \left[w_{i_{left}}, w_{i_{right}}\right],$$
$$r_{i_{left}}, r_{i_{right}} \in [0.1, 0.999999], w_{i_{left}}, w_{i_{right}}$$
$$\in [7.0, 12.0], n_i = (n_1, n_2, \ldots, n_{10}), 1 \leq n_i \leq 5$$

3) CRISP MORRAP FORMULATION

$$\text{Maximization } R_s(r, n) = \prod_{i=1}^{10} \left[1 - (1 - r_i)^{n_i}\right]$$

$$\text{Minimization } C_s(r, n) = \sum_{i=1}^{10} \left[\alpha_i \left(-\frac{1000}{\ln(r_i)}\right)^{1.5} \cdot (n_i + \exp(n_i/4))\right]$$

$$\text{Minimization } W_s(w, n) = \sum_{i=1}^{10} w_i . (n_i * exp(n_i/4))$$

$$\text{Subject to } \sum_{i=1}^{10} w_i v_i^2 n_i^2 \leq 289$$
$$0.5 \leq r_i \leq 1 - 10^{-5}, 1$$
$$\leq n_i \leq 5, 7.0 \leq w_i \leq 12.0$$
$$r_i = (r_1, r_2, \ldots, r_{10}), n_i = (n_1, \ldots, n_{10}), r_i$$
$$\in R, \quad 1 \leq n_i \leq 5.$$

The problems IT2FMORRAP, T1FMORRAP, and crisp MORRAP are solved using the proposed approach, as mentioned in Fig. 8. Specifically, the IT2FMORRAP will be

TABLE 3. Objectives solution of Pareto optimal set for MORRAP, T1FMORRAP, and IT2FMORRAP corresponding to 50, 100, 200, 400, 500, and 1000 iterations.

Itr. No.		MORRAP			T1FMORRAP			IT2FMORRAP		
		Maximum	Minimum	Average	Maximum	Minimum	Average	Maximum	Minimum	Average
50	R_S	0.99501	0.16807	0.754987	0.99501	0.16807	0.721284	**0.995010**	**0.168070**	**0.756789**
	C_S	701.907	50.30058	290.931	701.907	50.30058	282.3994	**701.9070**	**50.30058**	**277.4757**
	W_S	384.0529	36.25508	198.5205	327.149	64.13041	179.8324	**428.7591**	**77.06647**	**236.9000**
100	R_S	0.99501	0.16807	0.753555	0.99501	0.16807	0.71945	**0.995010**	**0.168070**	**0.735596**
	C_S	701.907	50.30058	295.1088	701.907	50.30058	278.879	**701.9070**	**50.30058**	**281.3898**
	W_S	387.3911	32.35902	195.4638	331.066	61.99837	182.3199	**434.5121**	**70.66489**	**239.2915**
200	R_S	0.99501	0.16807	0.750962	0.99501	0.16807	0.752123	**0.995010**	**0.168070**	**0.749557**
	C_S	701.907	50.30058	292.7743	701.907	50.30058	292.2811	**701.9070**	**50.30058**	**291.6494**
	W_S	375.5641	32.10064	194.5633	412.1878	35.95648	200.4407	**373.2623**	**36.47259**	**204.3371**
400	R_S	0.99501	0.16807	0.754442	0.99501	0.16807	0.75589	**0.995010**	**0.168070**	**0.749588**
	C_S	701.907	50.30058	295.349	701.907	50.30058	295.0742	**701.9070**	**50.30058**	**292.6684**
	W_S	386.6001	32.59213	197.8026	418.0858	32.10064	195.3253	**370.1533**	**32.10064**	**197.8944**
500	R_S	0.99501	0.16807	0.751306	0.99501	0.16807	0.755462	**0.995010**	**0.168070**	**0.753611**
	C_S	701.907	50.30058	290.9765	701.907	50.30058	294.4438	**701.9070**	**50.30058**	**293.2568**
	W_S	367.6624	32.10064	196.441	377.9323	32.10064	196.4905	**386.6790**	**32.10064**	**194.8376**
1000	R_S	0.99501	0.16807	0.750622	0.99501	0.16807	0.752036	**0.995010**	**0.168070**	**0.753611**
	C_S	701.907	50.30058	295.5739	701.907	50.30058	296.0336	**701.9070**	**50.30058**	**293.2568**
	W_S	384.2954	32.10064	197.1043	392.0788	32.10064	194.1505	**386.6790**	**32.10064**	**194.8376**

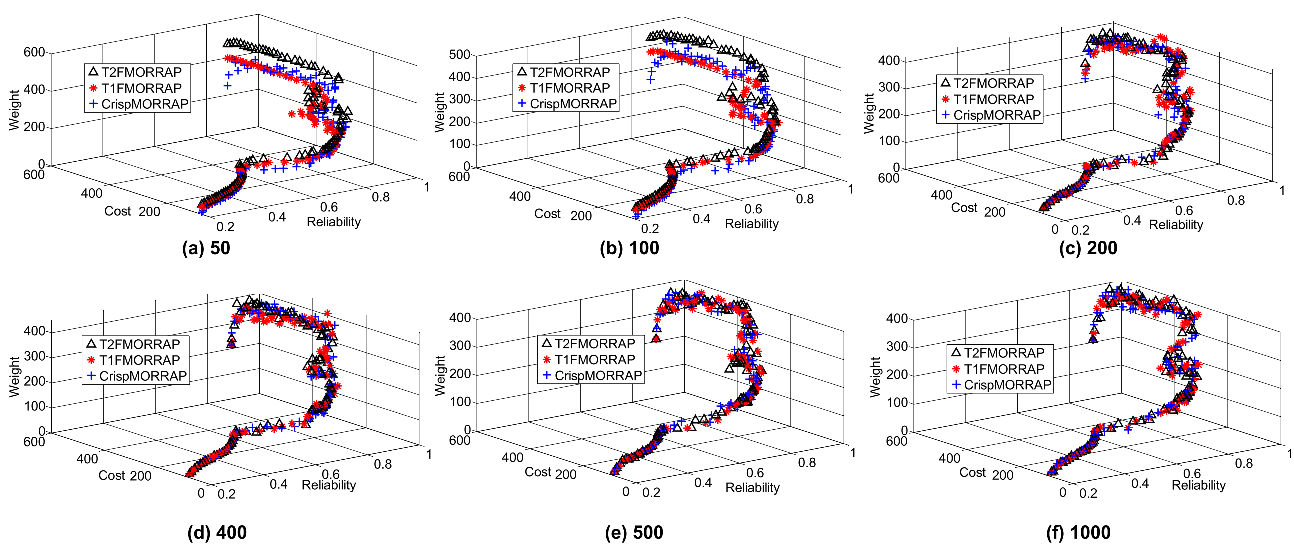

FIGURE 16. Pareto Front at (a) 50 iteration, (b) 100 iteration, (c) 200 iteration, (d) 400 iteration, (e) 500 iteration, and (f) 1000 iteration for IT2FMORRAP, T1FMORRAP, and Crisp MORRAOP.

solved using the IT2 fuzzy system with the component parameters, reliability, and weight as IT2FNs. The initial population passes through the IT2 fuzzy system, and the IT2 fuzzification, type-reduction, and defuzzification process take place, after that the NSGA-II procedures are applied to find the Pareto front for the IT2 fuzzy reliability, IT2 fuzzy cost, and IT2 fuzzy weight objectives. On the other hand, for solving the T1FMORRAP model, the proposed approach will utilize the T1 fuzzy system (T1 fuzzification and defuzzification process) for the generation of T1FNs corresponding to the reliability and weight components. Then, NSGA-II is applied to generate the Pareto front for the T1 fuzzy reliability, T1 fuzzy cost, and T1 fuzzy weight objectives. While, for solving the MORPAP model, the NSGA-II will directly apply as a multi-objective evolutionary optimization approach because there is no fuzziness involved

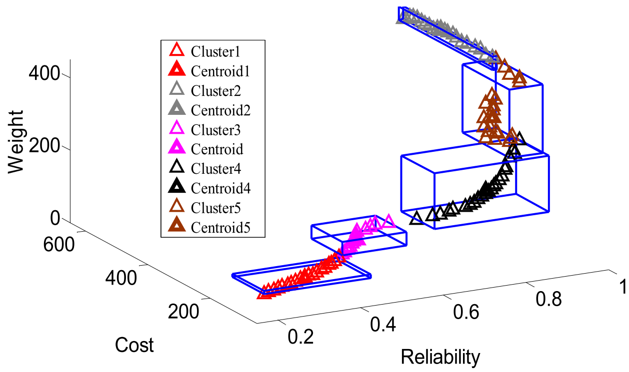

FIGURE 17. A typical illustration of different clusters obtained using K-mean for the Pareto optimal solution set for IT2FMORRAP at iteration 100.

in this scenario. It is mentioned that the reliability, weight, and number of redundant components are the decision variables in all three problems. The redundancy of a subsystem must always be an integer, so, at the time of evaluation, it has to be converted into the nearest integer value.

B. RESULTS AND DISCUSSION

The results are presented in the form of an optimal Pareto optimal set for the MORRAP, T1FMORRAP, and IT2FMORRAP corresponding to the different number of iterations. We have performed 50 runs for all the various instances of iterations and presented the suitable optimal set of solutions. It provides the support to justify the relative convergence and performances amongst the solution algorithms. The fitness function evaluation was conducted approximately 280 times, and the infeasibility for the individual solutions (for which the feasibility was not fulfilled). Moreover, with the initial population set to 100, approximately 200 individuals are created using genetic operations to form the mating pool. These individuals were sorted according to non-domination to have 100 final individuals ultimately.

The optimal Pareto-Fronts corresponding to the three approaches is shown in Fig. 16 for (a) 50, (b) 100, (c) 200, (d) 400, (e) 500, and (f) 1000 instances, respectively. Fig. 16 evidence that the Pareto optimal solutions for models converge as the iteration rises. From Fig. 16, we see that as the system's total reliability goes higher, its total cost and weight of the system become higher. For example, in iteration numbers 50 and 100, in Fig. 16 (a) and (b), respectively, there is a clear trade-off among the non-dominated outcomes represented by the IT2FMORRAP front than other approaches. So, the proposed IT2FMORRAP model has higher reliability and lower cost and weight function values. Further, there are tiny variations among the fronts when the numbers of iterations are 500 or more; see Fig. 16 (e) and (f). Thus, the IT2FMORRAP achieves a better front in a lesser iteration number. It means that the statistics of the Pareto optimal solutions are precisely noticeable at the lesser iteration number for IT2FMORRAP.

Table 3 illustrates the extreme and most minor boundaries of the generated optimal set of solutions for the IT2FMORRAP, T1FMORRAP, and MORRAP models. The lower (min) and upper (max) ranges of the total reliability, cost, and weight functions in the approaches are [0.168070, 0.99501], [50.300058, 701.9070], and [32.10064, 386.6790], respectively. The range and the non-dominated solutions in all three approaches are acceptable. As mentioned, all approaches were run 50 times; we have also said the mean of each objective value of the front in Table 3. From Table 3, the average of the total reliability function values of the IT2FMORRAP approach is higher than the other two approaches, and the cost values are lower for the smaller iteration number. However, the weight of the system is higher. Similarly, the IT2FMORRAP values are comparatively better for the other iteration number. It is to be noted that there is very little difference between the function values when the number of iterations is more significant. Therefore, the IT2MORRAP can be used as a conventional foundation to distinguish a single run's performance. We need to reduce the size of the solution sets to further deeply analyze the Pareto optimal solution sets for the three approaches. Since the decision-maker might have their own choices over selecting a particular individual solution, we have to use the data clustering approach to prune the optimal solutions. Moreover, we have used famous comparison metrics and statistical testing the compare the results.

C. CLUSTERING OF PARETO-FRONTS: K -MEAN CLUSTERING ALGORITHM

The next step is to prune solution sets after achieving acceptable Pareto-optimal solutions. One of the many significant purposes of shrinking the optimal solutions' size is to select meaningful solutions by decision-makers. Two strategies are designed to do the same, i.e., deciding based on the importance of the objective components with professional decision-makers and the data clustering technique. The first strategy is less fruitful than the decision-maker would hardly anticipate the analytical preference of the system's goals. However, the second approach of clustering to classify solutions in alternative domains and then decide the best solutions is relevant if there is an emphasis on their categorization. The use of the data clustering approach for reducing the size of an optimal set is presented in more detail in [45] and [66].

The k-mean identifies the best solution region of the Pareto-front from the three models. It offers excellent assistance for system designers investigating the variances between the three models. We used the silhouette plot strategy to evaluate the optimal number of clusters. This method calculates the allocation of objects to clusters to see if the groups are about the same quality (e.g., an equal number of objects in every collection). For example, Fig. 17 illustrates the clusters of Pareto optimal sets generated by IT2FMORRAP. There are two methods for identifying

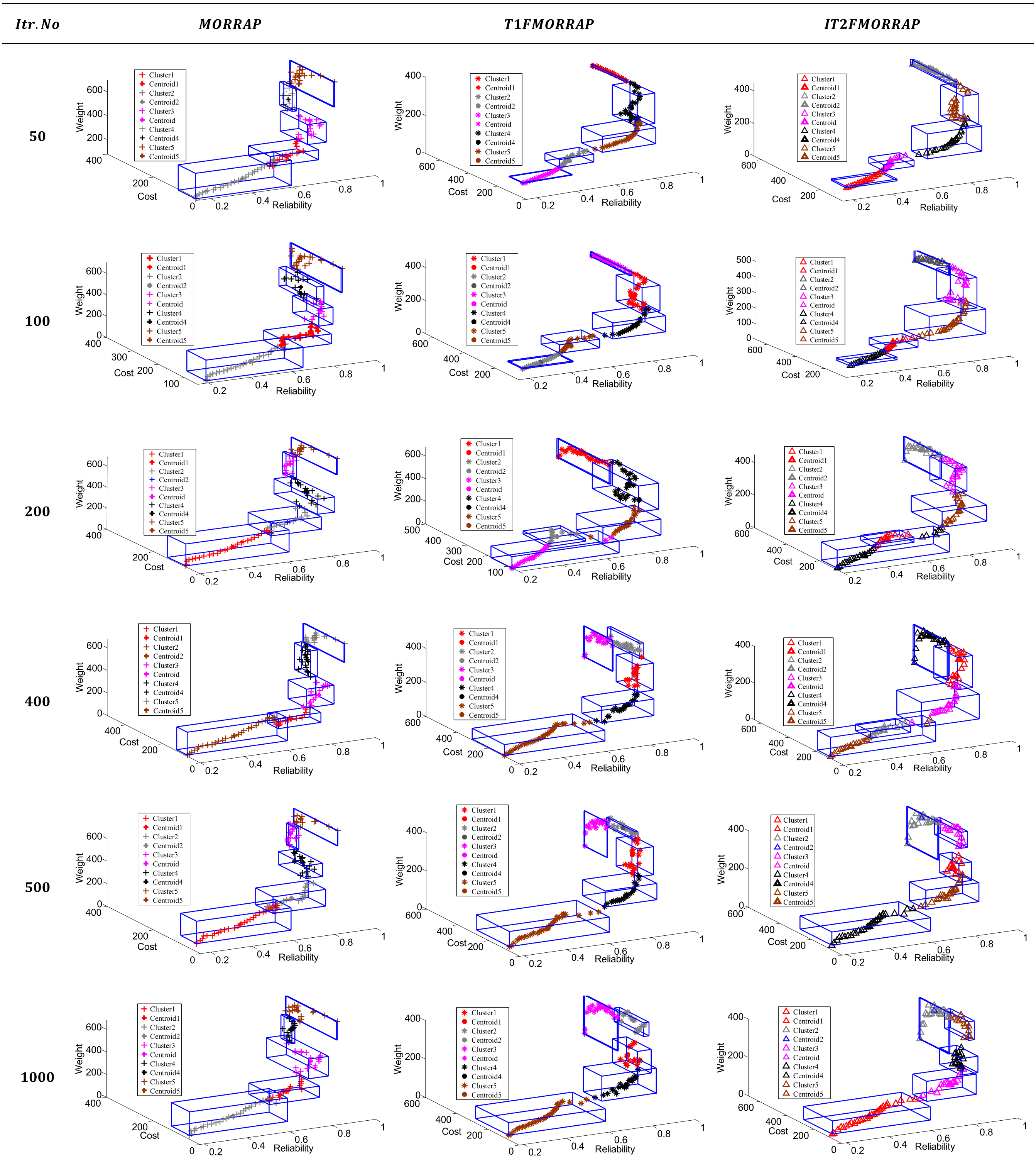

FIGURE 18. Pareto fronts with cluster center and centroids of the Pareto-Front found for various iterations of IT2FMORRAP, T1FMORRAP, and MORRAP.

the optimal solution among these five clusters. First, the cluster center (centroid) is calculated and considered the best representative solution. Second, the "knee" cluster is discovered since it includes the significantly superior Pareto solutions for trade-offs between the goals. The knee cluster is composed of the most impressive outcomes of the Pareto fronts, solutions where a minute increase in one goal would direct a considerable decline in at least one other

TABLE 4. Clustering results of Pareto-fronts obtained for MORRAP, T1FMORRAP, and IT2FMORRAP corresponding to 50, 100, 200, and 400 iterations.

No of iterations	Models	Clusters	No of Solutions	Reliability		Cost		Weight	
				Min	Max	Min	Max	Min	Max
50	Crisp MORRAP	**Cluster 1**	**19**	**0.647372**	**0.881989**	**138.8348**	**232.2369**	**108.0761**	**191.144**
		Cluster 2	31	0.168070	0.633636	36.25508	111.2945	50.30058	262.6119
		Cluster 3	17	0.873469	0.964490	178.6094	296.3860	197.3486	365.3174
		Cluster 4	14	0.969788	0.990602	329.5251	384.0529	306.8951	504.1913
		Cluster 5	19	0.990089	0.995010	169.5137	358.9774	492.3325	701.9070
	T1FMORRAP	Cluster 1	19	0.988076	0.990100	456.2500	552.9070	315.8460	326.9462
		Cluster 2	16	0.430568	0.603718	155.8606	257.8946	65.49992	107.1017
		Cluster 3	19	0.168070	0.417853	50.30058	147.8366	64.13041	67.23666
		Cluster 4	23	0.897661	0.986259	258.3841	430.4762	168.1147	327.1490
		Cluster 5	**23**	**0.618140**	**0.888452**	**116.4269**	**261.4892**	**127.3924**	**210.7934**
	IT2FMORRAP	Cluster 1	19	0.168070	0.425566	50.30058	152.1719	77.06647	86.41690
		Cluster 2	21	0.983958	0.995020	401.8207	552.9070	391.5078	428.2486
		Cluster 3	15	0.442343	0.596900	163.2062	262.5173	83.86066	121.1776
		Cluster 4	**23**	**0.616437**	**0.893620**	**99.80544**	**205.4074**	**155.6856**	**309.9325**
		Cluster 5	22	0.901187	0.981538	236.8216	387.6202	239.3791	428.7591
100	Crisp MORRAP	**Cluster 1**	**19**	**0.643708**	**0.873987**	**120.8309**	**195.9814**	**100.4277**	**194.1952**
		Cluster 2	31	0.168070	0.630833	32.35902	105.3701	50.30058	243.4352
		Cluster 3	13	0.882092	0.948864	174.9552	275.3443	196.6855	355.4798
		Cluster 4	15	0.954339	0.988772	241.6848	387.3911	288.1932	461.0629
		Cluster 5	22	0.989539	0.995010	176.8766	372.5829	477.9913	701.9070
	T1FMORRAP	Cluster 1	23	0.899806	0.985987	252.4763	419.6662	174.8504	331.0660
		Cluster 2	19	0.168070	0.412725	50.30058	144.6523	61.99837	67.82312
		Cluster 3	22	0.987722	0.995010	447.4229	552.9070	299.5581	325.5449
		Cluster 4	**17**	**0.636453**	**0.891631**	**91.27971**	**223.2731**	**141.2709**	**239.4774**
		Cluster 5	15	0.423513	0.618663	151.1107	270.6278	64.98785	116.7315
	IT2FMORRAP	Cluster 1	15	0.430668	0.601601	156.4053	267.2080	81.10574	125.9127
		Cluster 2	19	0.988796	0.990221	462.3199	552.9070	361.8377	434.5121
		Cluster 3	22	0.916641	0.987946	263.3563	447.7321	230.1616	424.9940
		Cluster 4	17	0.168070	0.413398	50.30058	145.6625	70.66489	86.79743
		Cluster 5	**27**	**0.615378**	**0.910405**	**97.11842**	**269.7705**	**141.4955**	**299.1701**
200	Crisp MORRAP	Cluster 1	32	0.168070	0.640126	32.10064	110.5197	50.30058	258.3915
		Cluster 2	**19**	**0.656110**	**0.882970**	**122.2660**	**223.5671**	**104.0805**	**219.8083**
		Cluster 3	15	0.975977	0.991778	330.6842	375.5641	336.1303	541.5902
		Cluster 4	19	0.892463	0.972634	148.6952	334.1131	213.4425	355.3240
		Cluster 5	15	0.992038	0.995010	158.7750	354.6400	550.7140	701.9070
	T1FMORRAP	Cluster 1	23	0.988333	0.995010	448.9022	552.9070	180.6826	351.0042
		Cluster 2	13	0.438388	0.607832	161.5149	282.8956	47.32428	73.14564
		Cluster 3	19	0.168070	0.655750	50.30058	151.3024	35.95648	138.0932
		Cluster 4	25	0.896537	0.987558	210.0843	433.8674	181.7252	412.1878
		Cluster 5	**20**	**0.623904**	**0.888100**	**93.77996**	**222.6883**	**89.30922**	**230.8093**
	IT2FMORRAP	Cluster 1	14	0.435135	0.619548	159.5773	250.2719	56.2314	87.03626
		Cluster 2	21	0.989376	0.996010	476.4906	5502.907	216.229	365.1702
		Cluster 3	21	0.932641	0.988875	310.7160	466.4728	223.3685	373.2623
		Cluster 4	23	0.168070	0.703905	50.30058	148.2601	36.47259	146.1264
		Cluster 5	**21**	**0.715473**	**0.928549**	**109.6834**	**300.8601**	**154.7671**	**252.3281**
400	Crisp MORRAP	**Cluster 1**	**14**	**0.643973**	**0.839024**	**102.6929**	**162.2072**	**92.44174**	**181.8273**
		Cluster 2	31	0.168070	0.625515	32.59213	88.96988	50.30058	253.0849
		Cluster 3	17	0.827310	0.953337	167.1641	265.7131	170.4436	336.7596
		Cluster 4	21	0.958941	0.991430	301.0579	386.6001	292.3553	527.7004
		Cluster 5	17	0.991699	0.995010	158.9724	379.1187	536.6238	701.9070
	T1FMORRAP	Cluster 1	16	0.898324	0.971252	222.9646	361.4529	187.2141	345.7779
		Cluster 2	15	0.974334	0.991345	316.4671	525.4060	329.0985	418.0858
		Cluster 3	18	0.991070	0.995010	516.6718	552.9070	158.7750	339.9589
		Cluster 4	**20**	**0.645962**	**0.886903**	**101.4946**	**226.3942**	**109.8173**	**206.8569**
		Cluster 5	31	0.168070	0.627052	50.30058	258.0575	32.10064	95.44486
	IT2FMORRAP	Cluster 1	22	0.914843	0.987693	267.0183	437.0619	191.7001	367.7944
		Cluster 2	14	0.426835	0.617911	153.4998	262.8927	50.51555	85.85374
		Cluster 3	**22**	**0.634086**	**0.909258**	**99.16308**	**278.3343**	**98.25722**	**232.7937**
		Cluster 4	23	0.988497	0.995010	453.0641	552.9070	159.9971	370.1533
		Cluster 5	19	0.168070	0.669955	50.30058	144.8031	32.10064	138.3264

objective. However, locating the knee area is challenging due to the unsystematic nature of the Pareto-fronts; hence, we have grouped all Pareto-solutions produced via various iterations.

TABLE 5. Clustering results of Pareto optimal sets obtained for MORRAP, T1FMORRAP, and IT2FMORRAP corresponding to 500, and 1000 iterations.

No of iterations	Models	Clusters	No of Solutions	Reliability		Cost		Weight	
				Min	Max	Min	Max	Min	Max
500	Crisp MORRAP	***Cluster 1***	31	0.168070	0.625233	32.10064	100.6030	50.30058	248.4446
		Cluster 2	**22**	**0.637810**	**0.891678**	**120.7502**	**194.7157**	**100.6624**	**249.0255**
		Cluster 3	16	0.981948	0.992176	324.0709	367.6624	364.2075	553.7988
		Cluster 4	18	0.901343	0.980146	211.2367	330.9491	245.7905	360.6048
		Cluster 5	13	0.992512	0.995010	158.7750	347.3708	567.1795	701.9070
	T1FMORRAP	*Cluster 1*	19	0.903245	0.97812	233.7644	372.7818	203.5062	350.6600
		Cluster 2	13	0.980591	0.991822	352.9828	540.9566	330.5843	377.9323
		Cluster 3	16	0.992175	0.995010	553.8434	552.9070	158.7750	344.9445
		Cluster 4	**21**	**0.650924**	**0.894404**	**97.03108**	**241.9577**	**143.1528**	**226.9026**
		Cluster 5	31	0.168070	0.636855	50.30058	263.5075	32.10064	111.5452
	IT2FMORRAP	*Cluster 1*	13	0.899063	0.958532	241.6212	366.616	164.6777	260.7254
		Cluster 2	19	0.990547	0.995010	501.7964	552.9070	158.7750	355.7887
		Cluster 3	16	0.962084	0.989883	310.4239	484.8635	303.5941	386.6790
		Cluster 4	31	0.168070	0.628905	50.30058	254.7127	32.10064	101.5604
		Cluster 5	**21**	**0.64349**	**0.890519**	**101.2971**	**206.4384**	**122.7636**	**221.4583**
1000	MORRAP	***Cluster 1***	**19**	**0.635003**	**0.870267**	**120.9375**	**207.4461**	**102.9232**	**203.6794**
		Cluster 2	31	0.168070	0.623581	32.10064	110.3548	50.30058	259.5443
		Cluster 3	18	0.880590	0.974240	177.4715	358.1153	204.6092	379.6899
		Cluster 4	15	0.977495	0.991484	337.2789	384.2954	320.0734	529.4631
		Cluster 5	17	0.991751	0.995010	158.7750	378.6018	538.5835	701.907
	T1FMORRAP	*Cluster 1*	13	0.897121	0.961682	229.4778	388.5894	153.7787	277.2986
		Cluster 2	14	0.965433	0.989321	282.3261	471.5641	322.0845	392.0788
		Cluster 3	21	0.989926	0.995010	485.9107	553.9070	158.7750	363.3329
		Cluster 4	**21**	**0.635765**	**0.888526**	**97.38103**	**214.9567**	**115.7271**	**245.2399**
		Cluster 5	31	0.168070	0.617898	50.30058	262.4468	32.10064	97.09964
	IT2FMORRAP	*Cluster 1*	31	0.168070	0.625053	50.30058	258.3743	32.10064	100.3309
		Cluster 2	21	0.989872	0.996010	484.1771	550.9070	158.7750	373.9964
		Cluster 3	**19**	**0.639759**	**0.871337**	**99.75023**	**201.5004**	**108.1655**	**213.2144**
		Cluster 4	15	0.880547	0.959599	224.8769	381.0006	161.3047	246.5654
		Cluster 5	14	0.962767	0.989356	297.7722	472.1872	302.0414	399.5519

The cluster in the knee region provides the individuals responsible for making decisions with a list of recommended alternatives from which they may choose the most appropriate solution. Fig. 18 demonstrates the cluster center, and centroids of the Pareto-Front found for various iterations (50, 100, 200, 400, 500, and 1000) concerning the IT2MORRAP, T1FMORRAP, and MORRAP. Fig. 18 demonstrates the clusters point along with the centroids of the Pareto Front for various iterations; 50, 100, 200, 400, 500, and 1000 for the IT2MORRAP, T1FMORRAP, and MORRAP. Moreover, the five representative ranges of solutions (corresponding to different clusters) are shown in Table 4 and Table 5. From Table 4 and Table 6, the expert chooses a solution region and analyzes the extreme objective function values. Once the clustering is done, we can further investigate the system objectives from Fig. 18 and Tables 4-5 as follows:

- For iteration number 50, as we can see from Fig. 18, the knee region solutions are formed by Cluster#4 with 23 numbers of solutions out of 100 for IT2FMORRAP. These pruned solutions are anticipated as important. The lower and upper values of the range for the goals (system reliability, cost, and weight values) of Cluster#4 corresponding to IT2FMORRAP are [0.616437, 0.89362], [99.80544, 205.4074], [155.6856, 309.9325] respectively (from Table 4). Cluster#1 and Cluster#5 are most likely in the knee region, with 19 and 23 numbers representative solutions for MORRAP and T1FMORRAP, respectively. The lower and upper values of the objective functions are [0.647972, 0.881989], [138.8348, 232.2369], and [1.8.191.144] for MORRAP and [0.61814, 0.888452], [116.4269, 261.4892], and [127.3924, 210.7934] for T1FMORRAP.
- Similarly, Cluster#5, with 27 representative solutions, is in the knee region for IT2FMORRAP with minimum and maximum reliability, cost, and weight values [0.615378, 0.910405], [97.11842, 269.7705], [141.4955, 299.1701], for 100 iterations. Also, Cluster#1 and Cluster#4 of MORRAP and T1FMORRAP are the knee clusters having 19 and 17 solutions with objective values ranges [0.643708, 0.873987], [120.8309, 195.9814], and [100.4277, 194.1952] and [0.636453, 0.891631], [91.27971, 223.2731], and [141.2709, 239.4774] respectively.
- For iteration number 200, the knee region cluster for IT2FMORRAP is Cluster#5 with 21 optimal solutions in it and the minimum and maximum reliability, cost, and weight values [0.715473, 0.928549], [109.6834, 300.8601], and [154.7671, 252.3281], Cluster#2 and Cluster#5 are the knee clusters having 19 and 20 solutions of MORRAP and T1FMORRAP with objective function values ranges [0.65611, 0.88297], [122.266, 223.5671], and [104.0805, 219.8083] and [0.623904,

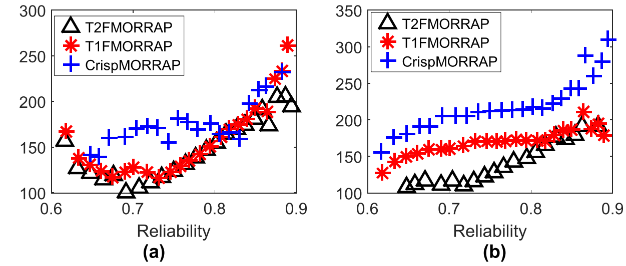

FIGURE 19. **Knee region cluster for 50 iterations. (a) Reliability vs. Cost (b) Reliability vs. weight.**

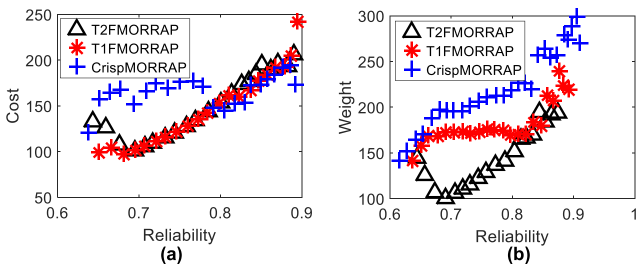

FIGURE 20. **Knee region cluster for 100 iterations. (a) Reliability vs. Cost (b) Reliability vs. weight.**

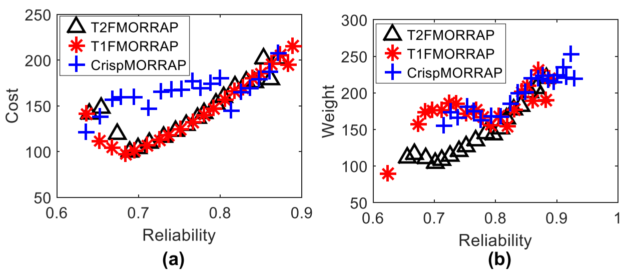

FIGURE 21. **Knee region cluster for 200 iterations. (a) Reliability vs. Cost (b) Reliability vs. weight.**

0.8881], [93.77996, 222.6883], and [89.30922, 230.8093] respectively.

The results mentioned above demonstrate that the designed IT2FMORRAP formulation archives better knee region solutions than the T1FMORRAP and MORRAP models for 50, 100, and 200 instances of iterations. The obtained amount of solutions of Cluster#4 for 50 instances, Cluster#5 for 100 instances, and Cluster#5 for 200 instances for IT2FMORRAP consisted of a higher number of solutions as achieved a more comprehensive range of objective values in comparison to the other two approaches. For 400, 500, and 1000 iterations, Cluster#3, Cluster#5, and Cluster#3 for IT2FMORRAP, respectively, are the most prominent solutions for decision-makers. When the numbers of instances are 500 or higher than it, the differences between the three approaches are minimal (see Table 5). This will again justify our argument that the IT2 fuzzy modeling of reliability optimization is more realistic and faster [21].

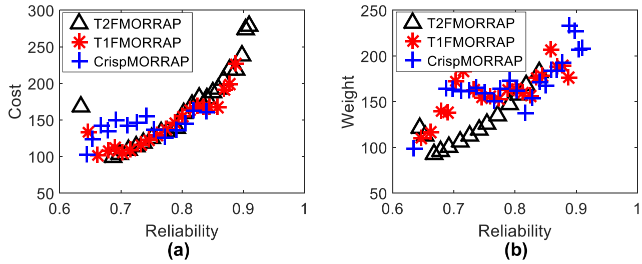

FIGURE 22. **Knee region cluster for 400 iterations. (a) Reliability vs. Cost (b) Reliability vs. weight.**

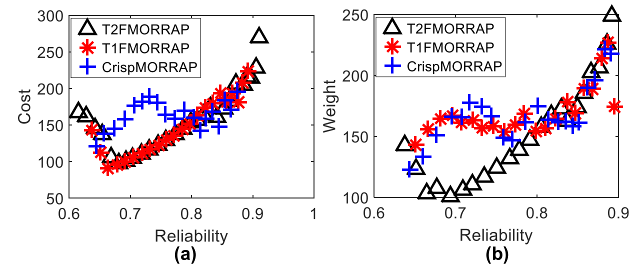

FIGURE 23. **Knee region cluster for 500 iterations. (a) Reliability vs. Cost (b) Reliability vs. weight.**

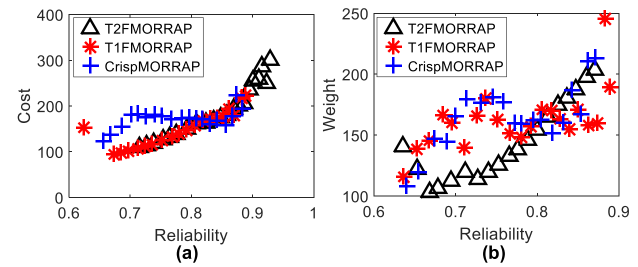

FIGURE 24. **Knee region cluster for 1000 iterations. (a) Reliability vs. Cost (b) Reliability vs. weight.**

Finally, the above results are plotted pairwise (a) reliability vs. cost and (b) reliability vs. weight objectives for illustration in Figs. 19–24 for 50, 100, 200, 400, 500, and 1000 iterations. This interpretation of the optimal solution sets can be useful to the decision-maker since it would have found suitable tradeoffs in the knee region.

In Fig. 19(a)-(b) for iteration 50, Clusters#1, Cluster#5, and Cluster#4 are considered for MORRAP, T1FMORRAP, and IT2FMORRAP, respectively, because they possess complete reliability vs. cost and reliability vs. weight of the system compared to the remaining clusters. Also, the IT2FMORRAP delivers the lowest values for cost and weight among the three clusters. Whereas in Fig. 20(a)-(b), Clusters#1 for MORRAP and Cluster#4 for T1FMORRAP have high reliability than Cluster#5 of IT2FMORRAP. However, it is accomplished at a relatively expensive cost and weight value. As mentioned earlier, in a similar context, solution clusters at the knee region in Fig. 21 to Fig. 24 reliability vs. cost and reliability vs. weight of the system compared. It can be easily observed that the IT2FMORRAP

TABLE 6. Computational results of six performance indicator.

Indicator	Model	Number of iterations					
		50	100	200	400	500	1000
NPS	MORRAP	95	97	95	97	98	97
	T1FMORRAP	97	100	99	99	100	99
	IT2FMORRAP	**100**	**100**	**100**	**100**	**100**	**100**
Diversity	MORRAP	7544487.614	8324472.177	11124123	12873628	8298307	8290319
	T1FMORRAP	7544487.614	8324472.177	11124123	**12873628**	8298307	10465564
	IT2FMORRAP	**8118979.543**	**11510789.95**	**12571945**	10358413	**8846262**	**10465564**
Spacing	MORRAP	8.568697896	7.657336906	10.08804	11.99424	13.08825	10.66079
	T1FMORRAP	**8.568697896**	**7.657336906**	**10.08804**	11.99424	13.08825	10.66079
	IT2FMORRAP	8.845039703	9.194494962	10.57608	**10.84046**	**11.15203**	**10.23500**
Spread	MORRAP	0.526489147	**0.441881425**	0.472299	**0.439115**	0.469793	0.468525
	T1FMORRAP	**0.456285575**	0.443066225	**0.44118**	0.501395	0.527824	0.478846
	IT2FMORRAP	0.464495046	0.464847601	0.475285	0.491037	**0.477641**	**0.456951**
HV	MORRAP	258254.9458	263315.7421	254788.9	262578.0	248976.6	261211.4
	T1FMORRAP	197757.6969	202064.6223	**279149.9**	**286066.7**	256530.9	266936.6
	IT2FMORRAP	**263848.9316**	**272361.4563**	250172.2	250808.9	**262964.7**	**272433.7**
NHV	MORRAP	0.661998394	0.674308592	0.721008	0.728914	0.73158	0.733504
	T1FMORRAP	0.650283527	0.656584574	0.728546	**0.736066**	**0.730198**	0.732403
	IT2FMORRAP	**0.723390087**	**0.731210022**	**0.729813**	0.730653	0.728491	**0.738121**

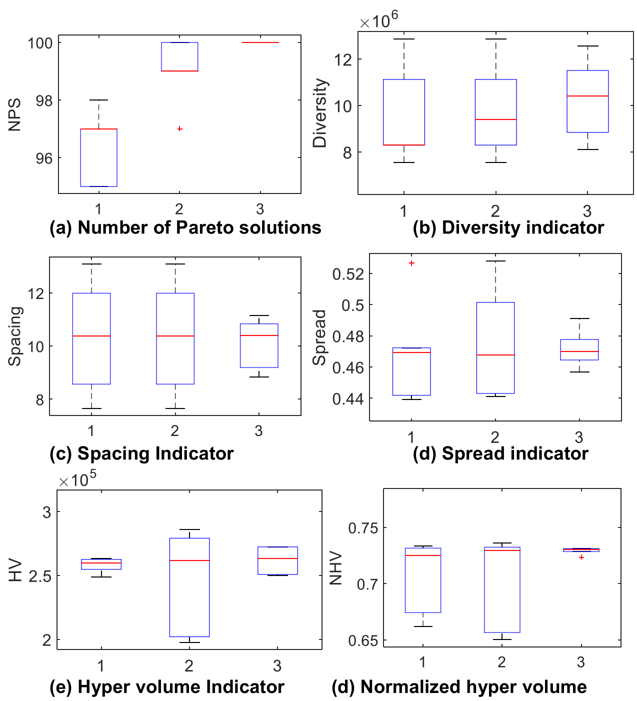

FIGURE 25. Performance indicators: for formulations (1) Crisp MORRAP, (2) T1FMORRAP, and (3) IT2FMORRAP.

cluster solutions outperform both T1FMORRAP and Crisp MORRAOP models by producing better Pareto solutions.

Although the trade-off solutions in the decision-making can only be confirmed as the most acceptable solution with knowing the decision preference, it is undoubtedly fascinating to point out the apparent and straightforward trade-off solution to three objectives higher than others and the final choice. Hence, the selection of one individual depends on the prospect of the decision-making and understanding of the system's needs, responsibilities, and expectations of the anticipated customer/users.

D. COMPUTATIONAL ILLUSTRATIONS OF PERFORMANCE INDICATORS

We have measured the number of Pareto solutions, diversity, spacing, spread, hyper volume, and normalized hyper volume performance indices [64] to compare the Pareto-fronts obtained from our experiments.

1) *The number of Pareto solutions (NPS):* It states that algorithm-I is better than algorithm-II; if algo-I generates P results and algo-II Q, provided $P > Q$.
2) *Diversity indicator* (D) : The D measures the diversity of the solution set:

$$D = \left[\sum_{i=1}^{N} \max \|x_i - y_i\|\right]^{1/2}$$

where, x_i and y_i are the two distinct non-dominated solutions of the optimal set.

1) *Spread indicator:* The spread values are calculated as.

$$Spread = \left[\sum_{m=1}^{M} \left(x_m^i - x_m^i\right)^2\right]^{1/2}$$

1) *Spacing indicator (SP):* The SP measures the relative distance among the consecutive solution points. SP is calculated using the following.

$$SP = \sqrt{\frac{\sum_{i=1}^{n} \left|d_i - \bar{d}\right|}{n}},$$
$$d_i = \sum\nolimits_{m=1}^{M} \left|x_m^i - x_m^j\right|, \bar{d} = \sum\nolimits_{i=1}^{n} \frac{d_i}{|n|}$$

TABLE 7. Simulation Samples of diversity for IT2FMORRAP, T1FMORRAP, and Crisp MORRAP.

Run	DM			Run	DM		
	MORRAP	T1FMORRAP	IT2FMORRAP		MORRAP	T1FMORRAP	IT2FMORRAP
1	11305147.47	9606194.659	9041814.813	26	12470287.12	8258727.839	8493239.444
2	8858033.705	12213786.63	11952421.39	27	9278097.602	7632372.82	9636659.255
3	9510217.72	10725560.71	9545934.147	28	9111411.548	9711093.746	9132216.728
4	9265633.749	9751659.764	10226692.73	29	9170431.462	9860459.563	8603297.782
5	10589461.59	8446492.725	13295646.46	30	9338021.25	8016100.11	10603810.3
6	9617103.854	7893874.132	9846556.682	31	10791766.52	8048107.486	11549984.84
7	11151724.29	8633585.367	9200087.102	32	11175292.17	8570009.375	12347909.3
8	9575088.786	8324613.461	10811957.26	33	8711732.481	9871785.079	8471701.697
9	8897797.786	9773876.538	8832689.808	34	8980218.14	8243724.262	9269965.181
10	8808756.876	7533073.672	9731681.146	35	7910324.409	6955307.373	10628549.56
11	9516365.484	7726842.076	8670113.54	36	9285405.039	10991100.79	9675385.612
12	9461043.952	8091352.018	10699980.88	37	10263884.33	7053280.987	12010719.7
13	10198800.44	8183017.688	10827389.73	38	10191881.1	8195563.314	9017471.946
14	11257294.48	9714887.632	11540760.76	39	8765062.57	8167082.824	9861235.292
15	8740534.831	9196433.772	9246720.855	40	11419876.8	9226732.754	10498813.1
16	10952397.31	7412155.787	9766019.527	41	9886376.937	7472143.027	10995109.48
17	11146923.47	7653939.689	9492185.049	42	10260159.4	9373397.451	10803003.24
18	8508859.292	7517667.05	9996595.998	43	9220297.246	8243014.271	9292006.079
19	9797647.478	8752101.643	9211044.118	44	9528713.446	8578530.792	8224931.589
20	13009565.05	9808692.014	8772664.718	45	10612278.49	8542330.059	9584299.306
21	9148241.52	7348340.95	9340794.989	46	9650372.34	11068089.64	9323281.596
22	9177204.879	8518814.71	12220073.74	47	10135235.29	7889995.996	9907616.815
23	10831162.98	7932101.754	9936299.42	48	9953813.478	8504674.244	11071571.6
24	9166322.28	7567319.149	10346454.15	49	9542918.219	7785131.029	8878564.41
25	11911175.34	7468836.022	10404754.79	50	11283671.71	8374384.512	8591671.548

1) *Hyper volume indicator (HV):* The HV measures the volume in the objective space covered by the non-dominated solutions. Mathematically, for individual solution i, a hypercube v_i is calculated with the reference point, constructed by the worst objective function values, and defined as follows:

$$HV = volume\left(\bigcup_{i=1}^{N} v_i\right)$$

1) *Normalized hyper volume indicator (NHV)*: The NHV calculates a normalized HV. It is the ratio of the volume of hypercube F for the current non-dominated solution to and the volume of hypercube F^* worst solution. Mathematically, defined as follows:

$$NHV = \frac{HV(F)}{HV(F^*)}$$

An algorithm with higher NPS, diversity, hypervolume and normalized hypervolume values (which means more diverse and non-dominated solutions) is better. However, an algorithm that gives smaller spacing and spread values solutions is best.

Using the mentioned indicators, we compare the solutions obtained from the three models: (1) IT2FMORRAP, (2) T1FMORRAP, and (3) Crisp MORRAP, at different instances of iterations. The measures were computed for three methods over the independent simulation of 50. Table 6 gives the numeric values of these indicators for 50, 100, 200, 400, 500, and 1000 instances.

Fig. 25 pictorially illustrates the critical observation for all indicators. It can be inferred from Fig. 25(a) that the mean of NPS in the established IT2FMORRAP process is greater than the other two methods, indicating the amount of non-dominated alternatives for IT2FMORRAP is more enormous than the MORRAP and T1FMORRAP. The mean of the diversity measure in the suggested IT2FMORRAP seems to have more relevance to other methods (see Fig. 25(b)). It implies that the IT2FMORRAP process has

TABLE 8. Tests of normality test diversity samples.

	Kolmogorov-Smirnov[a]			Shapiro-Wilk		
	Statistic	df	Sig.	Statistic	df	Sig.
MORRAP	0.148	50	0.008	0.946	50	0.023
T1FMORRAP	0.171	50	0.001	0.912	50	0.001
IT2FMORRAP	0.118	50	0.079	0.945	50	0.022

TABLE 9. Test of homogeneity test for diversity samples.

		Levene Statistic	df1	df2	Sig.
Diversity	Based on Mean	0.071	2	147	0.931
	Based on Median	0.088	2	147	0.916
	Based on Median and with adjusted df	0.088	2	146.079	0.916
	Based on trimmed mean	0.082	2	147	0.921

TABLE 10. Kruskal Wallis Test for Diversity Samples.

Rank			Statistics	
MODEL	N	Mean Rank	DM	
MORRAP	50	91	Chi-Square	40.446
T1FMORRAP	50	43.6	df	2
IT2FMORRAP	50	91.9	Asymp. Sig.	0.000
Total	150			

fewer non-convergences strategies for experimental tests. The average calculation of the spacing indicator (from Fig. 25 (c)) in the developed model is significantly smaller than other methods. That implies that the relative difference between the sequential non-dominated resolutions in the IT2FMORRAP is small. However, the suggested method's mean spread value has a much more significant effect than the T1FMORRAP and MORRAP (see Fig. 25 (d)). Fig. 25(e)-(f) shows that IT2FMORRAP produces non-dominated frameworks with significantly higher amounts for the hypervolume and normalized hypervolume measurements. Thus, the non-dominated results achieved mostly by the IT2FMORRAP approach are much more distributed equally than all those observed by other systems. Hence, IT2FMORRAP provides better representation in appearances of the NPS, diversity, spacing, HV, and NHV indicators compared with T1FMORRAP and crisp MORRAP.

E. STATISTICAL ANALYSIS

The statistical analysis has been given to evaluate the hypothesis about the results of the experimental investigation of the Pareto-fronts performance Viz. NPS, diversity, spacing, spread, HV, and NHV. Foremost, the data samples of performance metrics were checked to see if they were normal. After that, we compared the efficacy of IT2FMORRAP, T1FMORRAP, and Crisp MORRAP by analyzing the models with a 95% confidence level. Following are the assumptions considered for the normality, homogeneity, and comparison.

TABLE 11. Kruskal-Wallis Test for Spacing, Spread, HV, NHV and NPS.

	Ranks			Test Statistics		
	MODEL	N	Mean	Chi-Square	df	Asymp. Sig.
Spacing	MORRAP	50	94.06	39.940	2	0.000
	T1FMORRAP	50	43.96			
	T2FMORRAP	50	88.48			
Spread	MORRAP	50	85.36	14.085	2	0.001
	T1FMORRAP	50	56.68			
	T2FMORRAP	50	84.46			
HV	MORRAP	50	110.10	104.220	2	0.000
	T1FMORRAP	50	25.50			
	T2FMORRAP	50	90.90			
NHV	MORRAP	50	106.14	63.227	2	0.000
	T1FMORRAP	50	38.06			
	T2FMORRAP	50	82.30			
NPS	MORRAP	50	52.45	80.591	2	0.000
	T1FMORRAP	50	55.55			
	T2FMORRAP	50	118.50			

- Normality (Hypothesis 1): Sample data is insignificantly variated and normally distributed.
- Homogeneity (Hypothesis 2): Samples data follows the identical distribution of points.
- Comparison (Hypothesis 3): No significant difference in IT2FMORRAP, T1FMORRAP, and MORRAP on X, where X represents the vector of objectives.

Table 7 shows simulation samples of 50 runs for diversities of Pareto front generated by IT2FMORRAP, T1FMORRAP, and MORRAP, respectively. For the diversity data samples described in Table 7, Table 8 displays the results of a normality test directed employing the Kolmogorov-Smirnov and Shapiro-Wilk tests. In this test, we will use a sample size of 50 for each condition. The values considered significant (Sig.) are lower than 0.05. As a result, the normality test hypothesis (Hypothesis 1) is disproved. It denotes the diversity sample data deviation from the normal distribution. Table 9 shows the result of the Leven Test, which was used to test for homogeneity. Significant values, in this case, are more than 0.05. As a result, Hypothesis 2 is confirmed, pointing toward the samples being homogenous.

As earlier demonstrated, diverse data samples are typically not dispersed but relatively homogenous. As a result, the Kruskal-Wallis test is used to evaluate them. The statistical results for the Kruskal Wallis test are demonstrated in Table 11. In Table 12, diversity has a significant (Sig.) value of 0.000, less than 0.05, at a 5% significance threshold. As a result, rejecting the hypothesis (Hypothesis 3) demonstrates that samples vary greatly, showing the improved performance of the suggested IT2FMORRAP over T1FMORRAP and MORRAP for diversity.

Table 11 contains the statistical results of the Kruskal-Wallis test for different performance measures, including spacing, spread, NPS, HV, and NHV. The pattern mirrors that of Table 10. Thus, from Table 9 to Table 10, we prove that the proposed IT2FMORRAP considerably varies from T1FMORRAP and MORRAP on the performance metrics

TABLE 12. Comparison study of the proposed model with the well-known existing state-of-art models.

Authors	Structure	Multi-objectives	Target functions	Uncertain Parameters	Modeling approach	Algorithm	Solutions	Result
Wang et al. [46]	Deterministic	Two	R_S, C_S	$-non-$	Crisp numbers	NSGA-II	Pareto Front	$R_S = 0.9656$; $C_S = 235.3$.
Roy et al. [53]	Interval uncertain	Two	R_S, C_S	R & C	Interval-valued numbers	GA[1]	Single	$R_S = [0.9914, 0.9998]$; $C_S = [135.3863, 219.0110]$.
Sahoo et al. [51]	Interval uncertain	Two	R_S, C_S	R & C	Interval-valued numbers	GA[1]	Single	$R_S = [0.4625, 0.5175]$; $C_S = [71.9491, 120.6125]$.
Zhang et al. [52]	Interval uncertain	Two	R_S, C_S	R & C	Interval-valued numbers	MOPSO	Pareto Front	$R_S = [0.3162, 0.3566], [0.99994403, 0.99998972]$; $C_S = [2325.6, 2234.4], [13254, 13796]$.
Garg et al. [6]	T1 fuzzy uncertain	Two	R_S, C_S	R & C	T1 MFs	PSO[2]	Single	$R_S = 0.774142$; $C_S = 261.137251$.
Garg et al. [71]	Intuitionistic fuzzy uncertain	Two	R_S, C_S	R & C	Intuitionistic MFs	PSO[3]	Single	$R_S = (0.9978739, 0.9969936\ 0.9962003)$; $C_S = (391.45961, 375.41840, 367.95281)$.
Muhuri et al. [21]	T1 fuzzy uncertain	Two	R_S, C_S & R_S, W_S	r & c	T1 FNs	NSGA-II	Pareto Front	$R_S = [0.030148, 0.961686]$; $C_S = [11.2489, 551.1229]$.
Muhuri et al. [21]	IT2 fuzzy uncertain	Two	R_S, C_S & R_S, W_S	r & c	IT2 FNs	KM NSGA-II	Pareto Front	$R_S = [0.056188, 0.99299]$; $C_S = [13.71352, 552.9909]$.
Ashraf et al. [59]	IT2 fuzzy uncertain	Two	R_S, C_S	R & C	IT2 MFs	EKM -PSO[4]	Single	$R_S = 0.867611877$; $C_S = 437.0751367$
Taboada et al. [45]	Deterministic	Three	R_S, C_S, W_S	$-non-$	Real numbers	NSGA-II	Pareto Front	$R_S = 0.984265$; $CS = 15$; $WS = 25$.
Damghani et al. [69]	Deterministic	Three	R_S, C_S, W_S	$-non-$	Real numbers	DSAMOPSO	Pareto Front	$R_S = [0.999999999999211, 0.999999968973551]$ $C_S = [172, 276]$; $W_S = [101, 160]$.
Zhang et al. [70]	Deterministic	Three	R_S, C_S, W_S	$-non-$	Real numbers	BBMOPSO	Pareto Front	$R_S = [0.8069, 0.9977]$; $C_S = [18, 49]$; $W_S = [33, 78]$.
MORRAP	Deterministic	Three	R_S, C_S, W_S	$-non-$	Real numbers	NSGA-II	Pareto Front	$R_S = [0.130145, 0.9950]$; $C_S = [50.301, 551.907]$; $W_S = [35.96, 412.19]$.
T1FMORRAP	Type-1 fuzzy uncertain	Three	R_S, C_S, W_S	r, c & w	T1 FNs	EKM-NSGA-II	Pareto Front	$R_S = [0.130145, 0.9950]$; $C_S = [50.301, 551.907]$; $W_S = [35.96, 412.19]$.
Proposed IT2FMORRAP	IT2 fuzzy uncertain	Three	R_S, C_S, W_S	r, c & w	IT2 FNs	EKM-NSGA-II	Pareto-Front	$R_S = [0.16807, 0.9950]$; $C_S = [9.019947, 551.9275]$; $W_S = [83.8607, 428.25]$.

-non- represents that no parameters in the optimization model are uncertain.
[1]The two objectives are combined to make a single objective optimization problem and solved with the interval-valued GA.
[2]The two T1 fuzzy objectives are combined, and the corresponding crisp optimization problem is established to solve.
[3]The two Intuitionistic fuzzy objectives functions are combined, and the corresponding crisp optimization problem is established to solve.
[4]The two IT2 fuzzy objectives are combined, and the corresponding crisp optimization problem is established to solve.

considered. The findings of the hypothesis test, which are described in Table 11, support the validity of the inferences made from the experimental investigation.

F. CRITICAL ANALYSIS AND DISCUSSION

From the obtained results of the IT2FMORRAP, T1FMORRAP, and crisp MORRAP in Section VI (B-E), we found that IT2FMORRAP outperforms T1FMORRAP and crisp MORRAP in terms of the performance matrices. However, it is almost impossible to design and implement a high-performing system in a real-world scenario, as uncertainties are always present. Nowadays, the IT2FN is the most precise and renowned approach to epistemic uncertainties.

In summary, this work provides practical and indirect solutions to the decision-makers for finding the best optimal solution among the trade-off objectives of reliability, cost, and weight under the most suited environment. The K-mean clustering approach provides the best-suited region of the Pareto optimal set that helps the decision-makers to select an appropriate solution value of optimal reliability, cost, and weight according to their requirement. Further, the performance matrices, such as NPS, diversity, spacing, spread, HV, and NHV, express the superiority of the proposed IT2FMORRAP over the others.

VII. COMPARISON WITH THE WELL-KNOWN STATE OF ART MODELS

A comprehensive study of the proposed model with some well-known states of the art models is done here. The bibliographic literature on reliability optimization techniques is rich due to the popularity and applicability of the reliability issue. The researcher developed several single objectives and multi-objectives heuristics and meta-heuristics schemes to solve the problem. Moreover, there are different ways of managing the randomness and uncertainties: interval approach, probabilistic distributions, possibility theory, T1 fuzzy sets, intuitionistic fuzzy sets, and IT2 fuzzy set theories. Therefore, we have mainly focused on those related works in which the multiobjective optimization approaches are presented under the umbrella of uncertainties [3], [67], [68]. Table 12 shows a thorough comparative study of the proposed model with the well-known state-of-art models.

Wang et al. [46] addressed the MORRAP aiming the R_S maximization and C_S minimization with NSGA-II under the weight constraint concerning the component reliability and redundancies as crisp numbers. Khalil-Damghani et al. [69] presented a dynamically tuned multiobjective particle swarm approach for solving MORRAP with three objectives: R_S maximization, C_S minimization, and W_S minimization by finding the best-suited component reliability and redundancies for the series-parallel system. Taboada et al. [45] well-thought-out objectives, R_S maximization, C_S minimization, and W_S minimization in MORRAP and Pareto Front studies with the k-mean techniques. Zhang et al. [70] presented the barebones-based multiobjective PSO algorithm to address the three objectives (R_S, C_S, and W_S) MORRAP. Further, the authors have applied a sensitivity-based clustering technique to reduce the size of the optimal solution sets. In [45], [46], [69], and [70] deliberate the MORRAP, wherever indecision, hesitation, vagueness, and ambiguity in the featuring decision variables or parameters was not measured and therefore not appropriate to the practical-life systems. Sahoo et al. [51] solved IVMORRAP (interval-valued MORRAP) to maximize interval-valued reliability and cost functions using an entropy-based region-reducing GA. Roy et al. [53] considered the interval-valued reliability [R_{Left}, R_{right}], and interval-valued cost [C_{Left}, C_{right}] and proposed the IVMORRAP of the series-parallel system, then solved the proposed model using the GA algorithm.

Zhang et al. [52] formulated an IVMORRAP for the interval-valued reliability and cost functions. The authors introduced a multiobjective PSO algorithm to solve a SCADA system for water resources. Unfortunately, this is far from being a legitimate basis since considering an entire range of numbers (also known as an interval) to have equivalent probability is an uncommon occurrence in the existing natural system. Garg and Sharma [6] formulated a T1 fuzzy MORRAP for series-parallel systems using linear and non-linear membership functions corresponding to the system's reliability maximization and cost minimization objectives. The authors have used a de-fuzzified approach to establish a crisp model and solved it using a PSO algorithm. In [71], Garg et al. demonstrated intuitionistic fuzzy programming to design the reliability and cost functions of the system via the intuitionistic fuzzy membership functions with triangular interval data.

Recently, Muhuri et al. [21] presented the higher-order uncertainty associated with reliability components with IT2 fuzzy numbers and introduced an IT2FMORRAP model to two objectives: system reliability vs. cost and reliability vs. weight. The bi-objective IT2FMORRAP models are solved and compared with the T1 FN representations of parameters. In another work, Ashraf et al. [59] modeled the system reliability and cost functions with the interval-type-2 fuzzy membership functions by using Zadeh's extension principles and solving the formulated FMORRAP model using the EKM with particle swarm optimization algorithm. Therefore, no work has been considering the system's reliability, cost, and weight parameters with IT2 FNs to model the three objectives of IT2FMORRAP.

Therefore, we brought across our claims of rationales to prove those component parameters like reliability, cost, and weight, respectively, are much more practically formed with IT2 FNs than most other uncertainty designing methods, including T1 FNs or Interval-valued numbers [61], [62], [72]. Consequently, the work presented in this work is a general model of the MORRAP; almost all current MORRAP frameworks will be seen to be the exceptional circumstances of the presented IT2FMORRAP design.

VIII. CONCLUSION AND FUTURE WORKS

In this paper, an interval type-2 fuzzy multiobjective reliability redundancy allocation problem (IT2FMORRAP) under higher-order uncertainties in the system's reliability, cost, and weight parameters has been formulated. IT2FMORRAP considers three objectives: reliability, cost, and weight of a series-parallel system with parameters such as IT2FN. The underlining situations are established under which the proposed IT2FMORRAP model reduces to T1FMORRAP, IVMORRAP, and classical MORRAP. A novel solution approach is presented using the Enhance Karnik-Mendel algorithm and NSGA-II. Experimental simulations have been conducted using the pharmaceutical plant dataset to produce Pareto Fronts for all the considered models. The simulation reveals that the Pareto Fronts generated by IT2FMORRAP are superior to T1FMORRAP and crisp MORRAP. A k-mean clustering approach is employed to demonstrate the cluster center and centroids of the Pareto-Front found for various iterations 50, 100, 200, 400, 500, and 1000. Also, the five representative ranges of solutions corresponding to different clusters are shown. The most suited knee region cluster for IT2FMORRAP with 21 optimal solutions having the minimum and maximum reliability, cost, and weight values [0.715473, 0.928549], [109.6834, 300.8601], and [154.7671, 252.3281]. Similarly, the knee clusters having 19 and 20 solutions of MORRAP and T1FMORRAP with objective function values ranges [0.65611, 0.88297], [122.266, 223.5671], and [104.0805, 219.8083] and [0.623904, 0.8881], [93.77996, 222.6883], and [89.30922, 230.8093] respectively. The clusters at the knee region of the Pareto-front for two objectives (reliability vs. cost and reliability vs. weight) and three (reliability vs. cost vs. weight) are better for the proposed model compared to the other models for the all-considered iteration set with faster convergence for NSGA-II.

Moreover, the performance indicators Viz. the number of Pareto solutions, diversity, spacing, spread, hypervolume, and normalized hypervolume, indicate that the IT2FMORRAP model surpasses both considered models. Statistical analysis has also been conducted to compare the samples from the different runs of performance matrices. Kruskal Walli's test is used to confirm the hypothesis established in the experimental study. A simulation study and comparative performance analysis with other state-of-the-art methods from the literature have been conducted to find a suitable place for the proposed work in the domain.

As a limitation, we can observe that it is almost impossible to design and implement an exact optimal system in a real-world scenario with uncertainties. Therefore, for any solution model, continuous improvement is needed. Moreover, the characterization of both the epistemic and aleatory uncertainties simultaneously is still computationally challenging the researcher in practical applications.

The future direction will be considered as the use of General type-2 fuzzy number, Intuitionistic fuzzy number, and Interval type-2 Intuitionistic fuzzy number to represent the reliability, cost, and weight parameters of the MORRAP system. Further, some recent multi-objective meta-heuristics optimization algorithms may be used to solve the formulated model.

ACKNOWLEDGMENT

The author Zubair Ashraf would like to acknowledge the kind support from Prof. P. K. Muhuri and Dr. Q. M. Danish Lohani, Faculty of Mathematics and Computer Science, South Asian University, New Delhi.

AUTHOR CONTRIBUTIONS

Conceptualization: Zubair Ashraf; methodology: Zubair Ashraf and Mohammad Shahid; formal analysis and data curation: Zubair Ashraf and Mohammad Shahid; writing–original draft preparation: Zubair Ashraf, Mohammad Shahid, Faisal Ahmad, and Mohammad Sajid; writing–review and editing: Zubair Ashraf, Ketan Kotecha, Shruti Patil, Faisal Ahmad, and Mohammad Sajid; supervision: Zubair Ashraf, Mohammad Shahid, and Ketan Kotecha; funding: Ketan Kotecha. All authors have read and agreed to the published version of the manuscript.

CONFLICT OF INTEREST

The authors declare no conflict of interest.

DATA AVAILABILITY STATEMENT

Data can be provided only on request.

REFERENCES

[1] F. A. Tillman, C.-L. Hwang, and W. Kuo, "Determining component reliability and redundancy for optimum system reliability," *IEEE Trans. Rel.*, vol. R-26, no. 3, pp. 162–165, Aug. 1977, doi: 10.1109/TR.1977.5220102.

[2] W. Kuo and R. Wan, "Recent advances in optimal reliability allocation," *IEEE Trans. Syst., Man, A, Syst. Humans*, vol. 37, no. 2, pp. 143–156, Mar. 2007, doi: 10.1109/TSMCA.2006.889476.

[3] S. Devi, H. Garg, and D. Garg, "A review of redundancy allocation problem for two decades: Bibliometrics and future directions," *Artif. Intell. Rev.*, Dec. 2022, doi: 10.1007/s10462-022-10363-6.

[4] L. A. Zadeh, "Fuzzy sets," *Inf. Control*, vol. 8, no. 3, pp. 338–353, Jun. 1965, doi: 10.1016/S0019-9958(65)90241-X.

[5] V. Ravi, P. J. Reddy, and H. J. Zimmermann, "Fuzzy global optimization of complex system reliability," *IEEE Trans. Fuzzy Syst.*, vol. 8, no. 3, pp. 241–248, Jun. 2000, doi: 10.1109/91.855914.

[6] H. Garg and S. Sharma, "Multi-objective reliability-redundancy allocation problem using particle swarm optimization," *Comput. Ind. Eng.*, vol. 64, no. 1, pp. 247–255, Jan. 2013, doi: 10.1016/j.cie.2012.09.015.

[7] G. S. Mahapatra and T. K. Roy, "Optimal redundancy allocation in series-parallel system using generalized," *Tamsui Oxford J. Inf. Math. Sci.*, vol. 27, no. 1, pp. 1–20, 2011.

[8] O. Castillo, L. Amador-Angulo, J. R. Castro, and M. Garcia-Valdez, "A comparative study of type-1 fuzzy logic systems, interval type-2 fuzzy logic systems and generalized type-2 fuzzy logic systems in control problems," *Inf. Sci.*, vol. 354, pp. 257–274, Aug. 2016, doi: 10.1016/j.ins.2016.03.026.

[9] J. M. Mendel and D. Wu, *Perceptual Computing*. Hoboken, NJ, USA: Wiley, 2010, doi: 10.1002/9780470599655.

[10] L. A. Zadeh, "Fuzzy logic—A personal perspective," *Fuzzy Sets Syst.*, vol. 281, pp. 4–20, Dec. 2015, doi: 10.1016/j.fss.2015.05.009.

[11] L. A. Zadeh, "The concept of a linguistic variable and its application to approximate reasoning-I," *Inf. Sci.*, vol. 8, no. 3, pp. 199–249, 1975, doi: 10.1016/0020-0255(75)90036-5.

[12] J. M. Mendel and R. I. B. John, "Type-2 fuzzy sets made simple," *IEEE Trans. Fuzzy Syst.*, vol. 10, no. 2, pp. 117–127, Apr. 2002, doi: 10.1109/91.995115.

[13] J. M. Mendel, R. I. John, and F. Liu, "Interval type-2 fuzzy logic systems made simple," *IEEE Trans. Fuzzy Syst.*, vol. 14, no. 6, pp. 808–821, Dec. 2006, doi: 10.1109/TFUZZ.2006.879986.

[14] O. Castillo, P. Melin, J. Kacprzyk, and W. Pedrycz, "Type-2 fuzzy logic: Theory and applications," in *Proc. IEEE Int. Conf. Granul. Comput. (GRC)*, 2007, p. 145, doi: 10.1109/GrC.2007.118.

[15] J. M. Mendel and X. Liu, "Simplified interval type-2 fuzzy logic systems," *IEEE Trans. Fuzzy Syst.*, vol. 21, no. 6, pp. 1056–1069, Dec. 2013, doi: 10.1109/TFUZZ.2013.2241771.

[16] Z. Ashraf, M. L. Roy, P. K. Muhuri, and Q. M. Danish Lohani, "Interval type-2 fuzzy logic system based similarity evaluation for image steganography," *Heliyon*, vol. 6, no. 5, May 2020, Art. no. e03771, doi: 10.1016/j.heliyon.2020.e03771.

[17] L. Amador-Angulo and O. Castillo, "A new fuzzy bee colony optimization with dynamic adaptation of parameters using interval type-2 fuzzy logic for tuning fuzzy controllers," *Soft Comput.*, vol. 22, no. 2, pp. 571–594, Jan. 2018, doi: 10.1007/s00500-016-2354-0.

[18] T. Nguyen and S. Nahavandi, "Modified AHP for gene selection and cancer classification using type-2 fuzzy logic," *IEEE Trans. Fuzzy Syst.*, vol. 24, no. 2, pp. 273–287, Apr. 2016, doi: 10.1109/TFUZZ.2015.2453153.

[19] F. Gaxiola, P. Melin, F. Valdez, J. R. Castro, and O. Castillo, "Optimization of type-2 fuzzy weights in backpropagation learning for neural networks using GAs and PSO," *Appl. Soft Comput.*, vol. 38, pp. 860–871, Jan. 2016, doi: 10.1016/j.asoc.2015.10.027.

[20] K. Tai, A.-R. El-Sayed, M. Biglarbegian, C. Gonzalez, O. Castillo, and S. Mahmud, "Review of recent type-2 fuzzy controller applications," *Algorithms*, vol. 9, no. 2, p. 39, Jun. 2016, doi: 10.3390/a9020039.

[21] P. K. Muhuri, Z. Ashraf, and Q. M. D. Lohani, "Multi-objective reliability-redundancy allocation problem with interval type-2 fuzzy uncertainty," *IEEE Trans. Fuzzy Syst.*, vol. 26, no. 6, pp. 1339–1355, Jun. 2018, doi: 10.1109/TFUZZ.2017.2722422.

[22] P. Melin and O. Castillo, "A review on the applications of type-2 fuzzy logic in classification and pattern recognition," *Expert Syst. Appl.*, vol. 40, no. 13, pp. 5413–5423, Oct. 2013, doi: 10.1016/j.eswa.2013.03.020.

[23] Z. Ashraf, M. L. Roy, P. K. Muhuri, and Q. M. D. Lohani, "A novel image steganography approach based on interval type-2 fuzzy similarity," in *Proc. IEEE Int. Conf. Fuzzy Syst. (FUZZ-IEEE)*, Jul. 2018, pp. 1–8, doi: 10.1109/FUZZ-IEEE.2018.8491582.

[24] Z. Ashraf, D. Malhotra, P. K. Muhuri, and Q. M. Danish Lohani, "Interval type-2 fuzzy demand based vendor managed inventory model," in *Proc. IEEE Int. Conf. Fuzzy Syst. (FUZZ-IEEE)*, Jul. 2017, pp. 1–6, doi: 10.1109/FUZZ-IEEE.2017.8015738.

[25] Z. Ashraf, D. Malhotra, P. K. Muhuri, and Q. M. D. Lohani, "Interval type-2 fuzzy vendor managed inventory system and its solution with particle swarm optimization," *Int. J. Fuzzy Syst.*, vol. 23, no. 7, pp. 2080–2105, 2021, doi: 10.1007/s40815-021-01077-y.

[26] A. Amirkhani, M. Shirzadeh, and M. Molaie, "An indirect type-2 fuzzy neural network optimized by the grasshopper algorithm for vehicle ABS controller," *IEEE Access*, vol. 10, pp. 58736–58751, 2022, doi: 10.1109/ACCESS.2022.3179700.

[27] C. Wu and X. Guo, "A novel single fuzzifier interval type-2 fuzzy C-means clustering with local information for land-cover segmentation," *IEEE J. Sel. Topics Appl. Earth Observ. Remote Sens.*, vol. 14, pp. 5903–5917, 2021, doi: 10.1109/JSTARS.2021.3085606.

[28] Z. Ashraf and M. Shahid, "Multi-objective vendor managed inventory system with interval type-2 fuzzy demand and order quantities," *Int. J. Intell. Comput. Cybern.*, vol. 14, no. 3, pp. 439–466, Jul. 2021, doi: 10.1108/IJICC-12-2020-0212.

[29] M. Javanmard and H. M. Nehi, "A solving method for fuzzy linear programming problem with interval Type-2 fuzzy numbers," *Int. J. Fuzzy Syst.*, vol. 21, no. 3, pp. 882–891, Apr. 2019, doi: 10.1007/s40815-018-0591-3.

[30] D. W. Coit and A. E. Smith, "Reliability optimization of series-parallel systems using a genetic algorithm," *IEEE Trans. Rel.*, vol. 45, no. 2, pp. 254–260, Jun. 1996, doi: 10.1109/24.510811.

[31] Y. Nakagawa and K. Nakashima, "A heuristic method for determining optimal reliability allocation," *IEEE Trans. Rel.*, vol. R-26, no. 3, pp. 156–161, Aug. 1977, doi: 10.1109/TR.1977.5220101.

[32] M.-S. Chern, "On the computational complexity of reliability redundancy allocation in a series system," *Oper. Res. Lett.*, vol. 11, no. 5, pp. 309–315, 1992, doi: 10.1016/0167-6377(92)90008-Q.

[33] A. K. Dhingra, "Optimal apportionment of reliability and redundancy in series systems under multiple objectives," *IEEE Trans. Rel.*, vol. 41, no. 4, pp. 576–582, Dec. 1992, doi: 10.1109/24.249589.

[34] Z. Tian, M. J. Zuo, and H. Huang, "Reliability-redundancy allocation for multi-state series-parallel systems," *IEEE Trans. Rel.*, vol. 57, no. 2, pp. 303–310, Jun. 2008, doi: 10.1109/TR.2008.920871.

[35] L. D. S. Coelho, "An efficient particle swarm approach for mixed-integer programming in reliability–redundancy optimization applications," *Rel. Eng. Syst. Saf.*, vol. 94, no. 4, pp. 830–837, Apr. 2009, doi: 10.1016/j.ress.2008.09.001.

[36] W.-C. Yeh, Y.-C. Lin, Y. Y. Chung, and M. Chih, "A particle swarm optimization approach based on Monte Carlo simulation for solving the complex network reliability problem," *IEEE Trans. Rel.*, vol. 59, no. 1, pp. 212–221, Mar. 2010, doi: 10.1109/TR.2009.2035796.

[37] T.-J. Hsieh and W.-C. Yeh, "Penalty guided bees search for redundancy allocation problems with a mix of components in series–parallel systems," *Comput. Oper. Res.*, vol. 39, no. 11, pp. 2688–2704, Nov. 2012, doi: 10.1016/j.cor.2012.02.002.

[38] G. Kanagaraj, S. G. Ponnambalam, and N. Jawahar, "A hybrid cuckoo search and genetic algorithm for reliability–redundancy allocation problems," *Comput. Ind. Eng.*, vol. 66, no. 4, pp. 1115–1124, Dec. 2013, doi: 10.1016/j.cie.2013.08.003.

[39] L. D. Afonso, V. C. Mariani, and L. dos Santos Coelho, "Modified imperialist competitive algorithm based on attraction and repulsion concepts for reliability-redundancy optimization," *Expert Syst. Appl.*, vol. 40, no. 9, pp. 3794–3802, Jul. 2013, doi: 10.1016/j.eswa.2012.12.093.

[40] L. Wang and L.-P. Li, "A coevolutionary differential evolution with harmony search for reliability–redundancy optimization," *Expert Syst. Appl.*, vol. 39, no. 5, pp. 5271–5278, Apr. 2012, doi: 10.1016/j.eswa.2011.11.012.

[41] Z. Ashraf, M. Shahid, and F. Ahmad, "Gradient based optimization approach to solve reliability allocation system," in *Proc. Int. Conf. Comput., Commun., Intell. Syst. (ICCCIS)*, Feb. 2021, pp. 337–342, doi: 10.1109/ICCCIS51004.2021.9397197.

[42] D. W. Coit and A. Konak, "Multiple weighted objectives heuristic for the redundancy allocation problem," *IEEE Trans. Rel.*, vol. 55, no. 3, pp. 551–558, Sep. 2006, doi: 10.1109/TR.2006.879654.

[43] M. Sheikhalishahi, V. Ebrahimipour, H. Shiri, H. Zaman, and M. Jeihoonian, "A hybrid GA-PSO approach for reliability optimization in redundancy allocation problem," *Int. J. Adv. Manuf. Technol.*, vol. 68, pp. 317–338, Sep. 2013, doi: 10.1007/s00170-013-4730-6.

[44] H. A. Taboada, J. F. Espiritu, and D. W. Coit, "MOMS-GA: A multi-objective multi-state genetic algorithm for system reliability optimization design problems," *IEEE Trans. Rel.*, vol. 57, no. 1, pp. 182–191, Mar. 2008, doi: 10.1109/TR.2008.916874.

[45] H. A. Taboada, F. Baheranwala, D. W. Coit, and N. Wattanapongsakorn, "Practical solutions for multi-objective optimization: An application to system reliability design problems," *Rel. Eng. Syst. Saf.*, vol. 92, no. 3, pp. 314–322, Mar. 2007, doi: 10.1016/j.ress.2006.04.014.

[46] Z. Wang, T. Chen, K. Tang, and X. Yao, "A multi-objective approach to redundancy allocation problem in parallel-series systems," in *Proc. IEEE Congr. Evol. Comput.*, May 2009, pp. 582–589, doi: 10.1109/CEC.2009.4982998.

[47] D. Salazar, C. M. Rocco, and B. J. Galván, "Optimization of constrained multiple-objective reliability problems using evolutionary algorithms," *Rel. Eng. Syst. Saf.*, vol. 91, no. 9, pp. 1057–1070, Sep. 2006, doi: 10.1016/j.ress.2005.11.040.

[48] A. Zaretalab, V. Hajipour, M. Sharifi, and M. R. Shahriari, "A knowledge-based archive multi-objective simulated annealing algorithm to optimize series–parallel system with choice of redundancy strategies," *Comput. Ind. Eng.*, vol. 80, pp. 33–44, Feb. 2015, doi: 10.1016/j.cie.2014.11.008.

[49] D. Cao, A. Murat, and R. B. Chinnam, "Efficient exact optimization of multi-objective redundancy allocation problems in series-parallel systems," *Rel. Eng. Syst. Saf.*, vol. 111, pp. 154–163, Mar. 2013, doi: 10.1016/j.ress.2012.09.013.

[50] R. K. Gupta, A. K. Bhunia, and D. Roy, "A GA based penalty function technique for solving constrained redundancy allocation problem of series system with interval valued reliability of components," *J. Comput. Appl. Math.*, vol. 232, no. 2, pp. 275–284, Oct. 2009, doi: 10.1016/j.cam.2009.06.008.

[51] L. Sahoo, A. K. Bhunia, and P. K. Kapur, "Genetic algorithm based multi-objective reliability optimization in interval environment," *Comput. Ind. Eng.*, vol. 62, no. 1, pp. 152–160, Feb. 2012, doi: 10.1016/j.cie.2011.09.003.

[52] E. Zhang and Q. Chen, "Multi-objective reliability redundancy allocation in an interval environment using particle swarm optimization," *Rel. Eng. Syst. Saf.*, vol. 145, pp. 83–92, Jan. 2016, doi: 10.1016/j.ress.2015.09.008.

[53] P. Roy, B. S. Mahapatra, G. S. Mahapatra, and P. K. Roy, "Entropy based region reducing genetic algorithm for reliability redundancy allocation in interval environment," *Expert Syst. Appl.*, vol. 41, no. 14, pp. 6147–6160, Oct. 2014, doi: 10.1016/j.eswa.2014.04.016.

[54] V. Ebrahimipour and M. Sheikhalishahi, "Application of multi-objective particle swarm optimization to solve a fuzzy multi-objective reliability redundancy allocation problem," in *Proc. IEEE Int. Syst. Conf.*, Apr. 2011, pp. 326–333, doi: 10.1109/SYSCON.2011.5929085.

[55] J. Guo, Z. Wang, M. Zheng, and Y. Wang, "Uncertain multiobjective redundancy allocation problem of repairable systems based on artificial bee colony algorithm," *Chin. J. Aeronaut.*, vol. 27, no. 6, pp. 1477–1487, Dec. 2014, doi: 10.1016/j.cja.2014.10.014.

[56] Z. Ashraf, P. K. Muhuri, Q. M. Danish Lohani, and R. Nath, "Fuzzy multi-objective reliability-redundancy allocation problem," in *Proc. IEEE Int. Conf. Fuzzy Syst. (FUZZ-IEEE)*, Jul. 2014, pp. 2580–2587, doi: 10.1109/FUZZ-IEEE.2014.6891889.

[57] Z. Ashraf, P. K. Muhuri, and Q. M. D. Lohani, "Particle swam optimization based reliability-redundancy allocation in a type-2 fuzzy environment," in *Proc. IEEE Congr. Evol. Comput. (CEC)*, May 2015, pp. 1212–1219, doi: 10.1109/CEC.2015.7257027.

[58] B. N. Chebouba, M. A. Mellal, and S. Adjerid, "Fuzzy multiobjective system reliability optimization by genetic algorithms and clustering analysis," *Qual. Rel. Eng. Int.*, vol. 37, no. 4, pp. 1484–1503, Jun. 2021, doi: 10.1002/qre.2809.

[59] Z. Ashraf, P. K. Muhuri, Q. M. D. Lohani, and M. L. Roy, "Type-2 fuzzy reliability–redundancy allocation problem and its solution using particle-swarm optimization algorithm," *Granular Comput.*, vol. 4, no. 2, pp. 145–166, Apr. 2019, doi: 10.1007/s41066-018-0106-5.

[60] W. Kuo and V. R. Prasad, "An annotated overview of system-reliability optimization," *IEEE Trans. Rel.*, vol. 49, no. 2, pp. 176–187, Jun. 2000, doi: 10.1109/24.877336.

[61] H. Bustince, E. Barrenechea, M. Pagola, J. Fernandez, Z. Xu, B. Bedregal, J. Montero, H. Hagras, F. Herrera, and B. De Baets, "A historical account of types of fuzzy sets and their relationships," *IEEE Trans. Fuzzy Syst.*, vol. 24, no. 1, pp. 179–194, 2015.

[62] H. B. Sola, J. Fernandez, H. Hagras, F. Herrera, M. Pagola, and E. Barrenechea, "Interval type-2 fuzzy sets are generalization of interval-valued fuzzy sets: Toward a wider view on their relationship," *IEEE Trans. Fuzzy Syst.*, vol. 23, no. 5, pp. 1876–1882, Oct. 2015, doi: 10.1109/TFUZZ.2014.2362149.

[63] K. Deb, A. Pratap, S. Agarwal, and T. Meyarivan, "A fast and elitist multiobjective genetic algorithm: NSGA-II," *IEEE Trans. Evol. Comput.*, vol. 6, no. 2, pp. 182–197, Apr. 2002, doi: 10.1109/4235.996017.

[64] K. Deb, *Multi-Objective Optimization Using Evolutionary Algorithms*. New York, NY, USA: Wiley, 2001.

[65] M. M. Raghuwanshi and O. G. Kakde, "Survey on multiobjective evolutionary and real coded genetic algorithms," in *Proc. Asia Pacific Symp. Intell. Evol. Syst.*, vol. 1984, 2004, pp. 150–161. [Online]. Available: http://www.complexity.org.au/cgi-bin/conference/accepted_paper.cgi?paperid=raghuw01

[66] H. A. Taboada and D. W. Coit, "Data clustering of solutions for multiple objective system reliability optimization problems," *Qual. Technol. Quantum Manag.*, vol. 4, no. 2, pp. 191–210, Feb. 2007, doi: 10.1080/16843703.2007.11673145.

[67] S. Nannapaneni and S. Mahadevan, "Reliability analysis under epistemic uncertainty," *Rel. Eng. Syst. Saf.*, vol. 155, pp. 9–20, Nov. 2016, doi: 10.1016/j.ress.2016.06.005.

[68] E. Zio, "Reliability engineering: Old problems and new challenges," *Rel. Eng. Syst. Saf.*, vol. 94, no. 2, pp. 125–141, Feb. 2009, doi: 10.1016/j.ress.2008.06.002.

[69] K. Khalili-Damghani, A.-R. Abtahi, and M. Tavana, "A new multi-objective particle swarm optimization method for solving reliability redundancy allocation problems," *Rel. Eng. Syst. Saf.*, vol. 111, pp. 58–75, Mar. 2013, doi: 10.1016/j.ress.2012.10.009.

[70] E. Zhang, Y. Wu, and Q. Chen, "A practical approach for solving multi-objective reliability redundancy allocation problems using extended bare-bones particle swarm optimization," *Rel. Eng. Syst. Saf.*, vol. 127, pp. 65–76, Jul. 2014, doi: 10.1016/j.ress.2014.03.006.

[71] H. Garg, M. Rani, S. P. Sharma, and Y. Vishwakarma, "Intuitionistic fuzzy optimization technique for solving multi-objective reliability optimization problems in interval environment," *Expert Syst. Appl.*, vol. 41, no. 7, pp. 3157–3167, Jun. 2014, doi: 10.1016/j.eswa.2013.11.014.

[72] D. Dubois and H. Prade, "The legacy of 50 years of fuzzy sets: A discussion," *Fuzzy Sets Syst.*, vol. 281, pp. 21–31, Dec. 2015, doi: 10.1016/j.fss.2015.09.004.

ZUBAIR ASHRAF received the master's degree in computer science and applications from Aligarh Muslim University, Aligarh, India, in 2013, and the Ph.D. degree in computer science from South Asian University, New Delhi, India, in 2020. He is currently an Assistant Professor with the Department of Computer Engineering and Application, GLA University, Mathura, Uttar Pradesh, India. His research interests include machine learning, evolutionary optimization, nature-inspired intelligent computation, deep learning, and fuzzy systems. He is an IEEE Young Professional and an active member of several societies, including the IEEE Computational Intelligence Society and EUSFLAT. He is also an active Reviewer of journals, such as IEEE TRANSACTIONS ON FUZZY SYSTEMS, *Soft Computing*, *Applied Soft Computing*, *Applied Mathematics*, and the *International Journal of Intelligence Systems*.

MOHAMMAD SHAHID (Member, IEEE) received the M.Tech. and Ph.D. degrees from the School of Computer and Systems Sciences, Jawaharlal Nehru University, New Delhi, India, and the M.C.A. degree from the Department of Computer Science, Aligarh Muslim University, Aligarh, India. He is currently an Assistant Professor of computer science with the Department of Commerce, Aligarh Muslim University. He has published many research papers in international conferences and journals of repute (including Elsevier, Springer, Inderscience, Wiley, Taylor & Francis, IGI Global, and IEEE). His research interests include grid/cloud computing, workflow scheduling, evolutionary computing, meta-heuristic optimization, and portfolio optimization. He was awarded the Research Startup Grant from UGC-BSR, India, in 2017.

FAISAL AHAMD received the M.C.A. degree from Aligarh Muslim University, in 2009, and the Ph.D. degree in software engineering from NIT Durgapur, India, in 2019. He is currently a Senior Software Engineer with Workday Inc., USA. He has 14 years of industrial experience in different roles from developer to architect role. He has published papers in international journals along with many international and national conferences. His current research interests include cloud computing, software engineering, machine learning, and portfolio optimization. He is also a reviewer of many international journals.

MOHAMMAD SAJID received the M.C.A., M.Tech., and Ph.D. degrees from the School of Computer and Systems Sciences, Jawaharlal Nehru University (JNU), New Delhi. He is currently an Assistant Professor with the Department of Computer Science, Aligarh Muslim University, India. He has published many research papers in international conferences and international journals of repute. His research interests include parallel and distributed computing, cloud computing, evolutionary and swarm intelligence algorithms, and combinatorial optimization problems. He was awarded a research startup grant (ten lakhs) from UGC-BSR, India, in 2017.

KETAN KOTECHA is currently an administrator and a teacher of deep learning. He has expertise and experience in cutting-edge research and projects in AI and deep learning for the last 25 years. He has widely published with more than 100 publications in several excellent peer-reviewed journals on various topics ranging from cutting-edge AI, education policies, teaching-learning practices, and AI for all. He has published three patents and delivered keynote speeches at various national and international forums, including the Machine Intelligence Laboratory, USA, IIT Bombay under the World Bank Project, and the International Indian Science Festival organized by the Department of Science and Technology, Government of India. His research interests include artificial intelligence, computer algorithms, machine learning, and deep learning. He was a recipient of the two SPARC projects in AI worth INR 166 lakhs from MHRD, Government of India, in collaboration with the Arizona Mobility Grant to Poland, the DUO–India Professors Fellowship for research in responsible AI in collaboration with Brunel University, U.K., the LEAP Grant by Cambridge University, U.K., the UKIERI Grant by Aston University, USA, and The University of Queensland, Australia. He was also a recipient of numerous prestigious awards, such as Erasmus+ Faculty U.K., and a grant from the Royal Academy of Engineering, U.K., under Newton Bhabha Fund. He is an Academic Editor of *Computer Science* (PeerJ) and an Associate Editor of IEEE ACCESS.

SHRUTI PATIL received the M.Tech. degree in computer science and the Ph.D. degree in data privacy from Pune University. She has been an industry professional in the past. She is currently associated with the Symbiosis Institute of Technology as a Professor and with SCAAI, Pune, Maharashtra, as a Research Associate. She has three years of industry experience and ten years of academic experience. She has expertise in applying innovative technology solutions to real-world problems. She is also working in the application domains of healthcare, sentiment analysis, emotion detection, and machine simulation, via which she is also guiding several bachelor's, master's, and Ph.D. students as domain experts. She has published more than 30 research papers in reputed international conferences and Scopus Web of Science indexed journals and books. Her research interests include applied artificial intelligence, natural language processing, acoustic AI, adversarial machine learning, data privacy, digital twin applications, GANS, and multimodal data analysis.